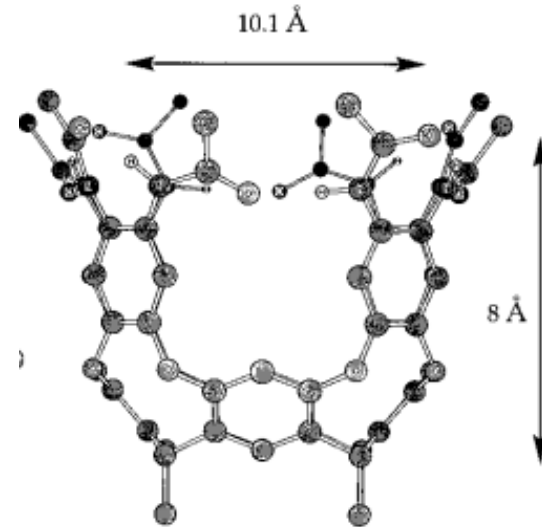
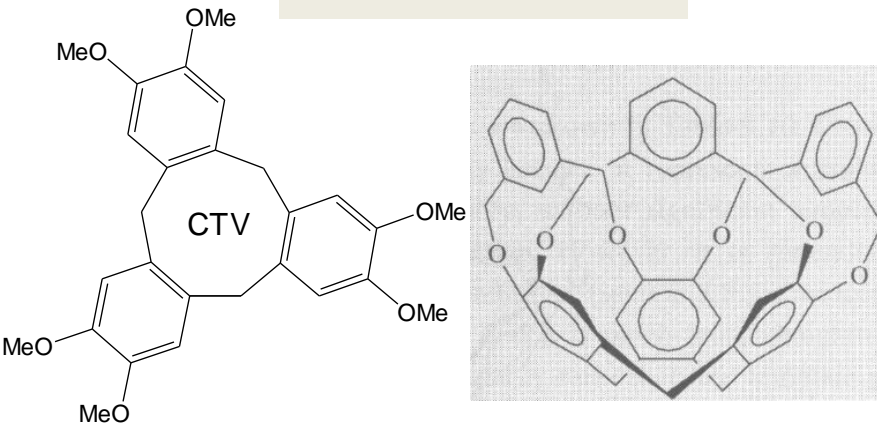
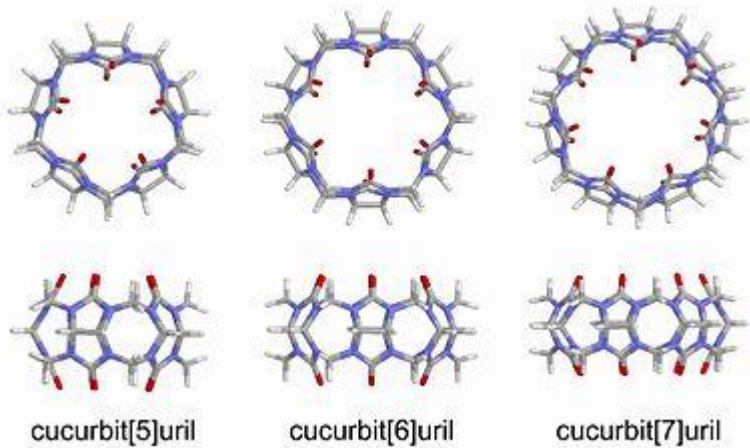


Cavitandi

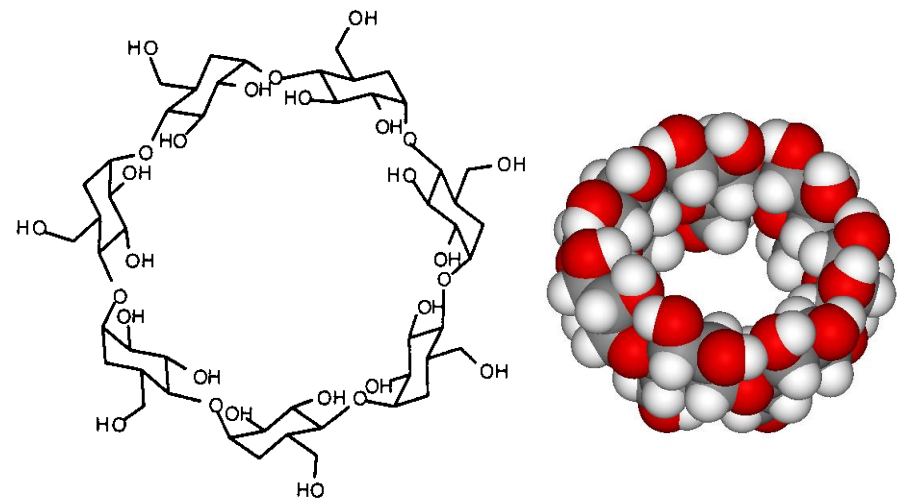
ciclotriveratrilene



Cucurbiturili



Ciclodestrine



Capsule Molecolari

Unione di due cavitandi

Connessione covalente

Legame idrogeno

Legame di coordinazione

Pre-organizzazione

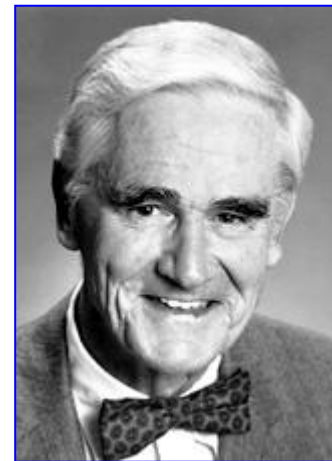
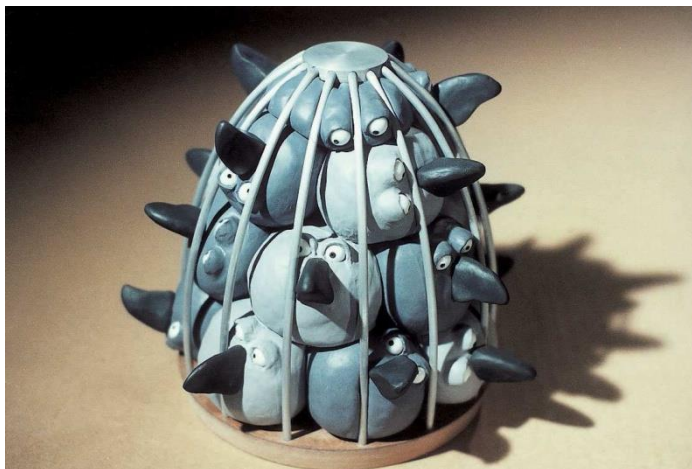
Protezione dal solvente esterno

Rallentamento delle cinetiche di scambio

Stabilizzazione di specie reattive

Reazioni catalitiche

Drug delivery

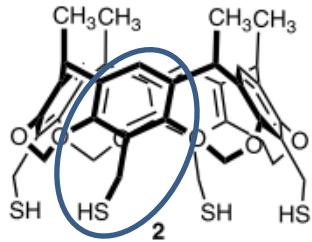


Carcerando:

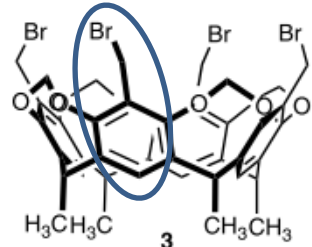
Contenitore molecolare chiuso (capsula) che definisce cavità sferica, i guest sono intrappolati (all'atto della sintesi) entrata e uscita solo per rottura di legame covalente, i.e. velocità di scambio virtualmente nulla

Carcerandi

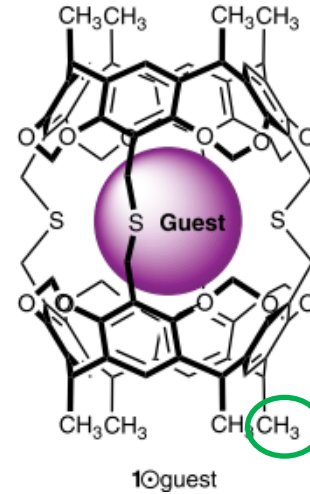
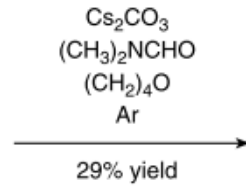
Benzil-tiolo



benzil cloruro
(o bromuro)

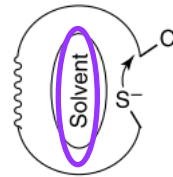
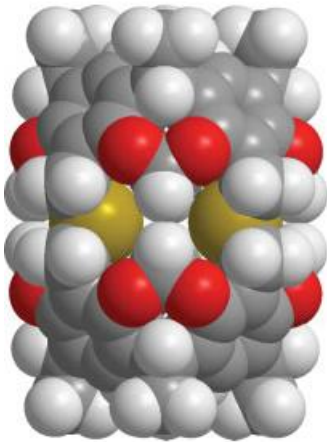


Alta dliuz



Guest: Cs^+ ; $(\text{CH}_3)_2\text{NCHO}$;
 $(\text{CH}_2)_4\text{O}$; Ar

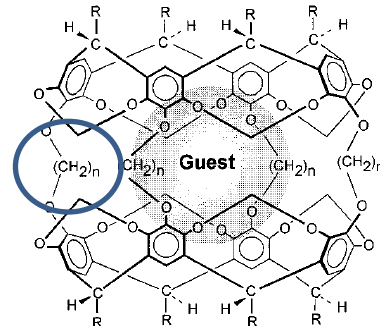
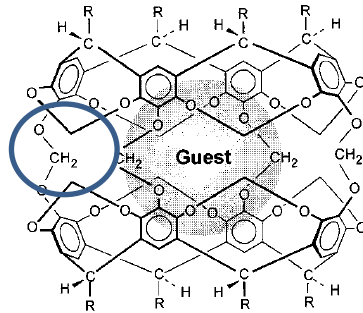
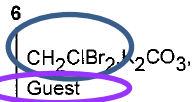
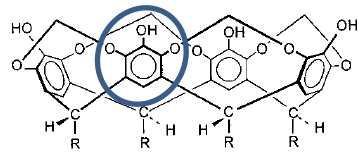
Insolubilità = caratterizz via IR, FAB-MS, analisi elementare, test chimici
FAB-MS dei carciplessi



Carcerandi

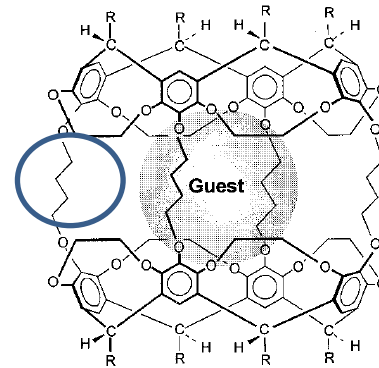
fenolo

bromo-clorometano

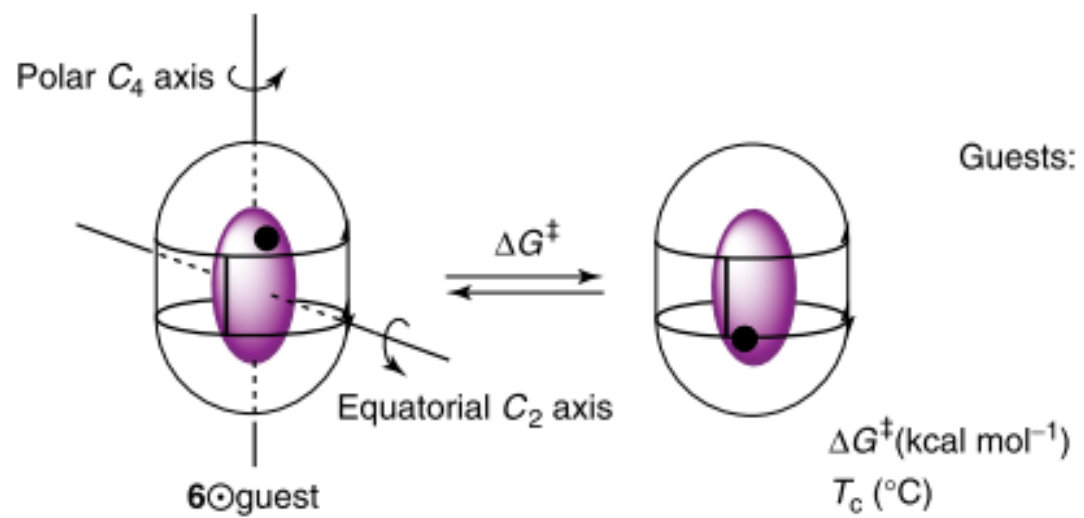


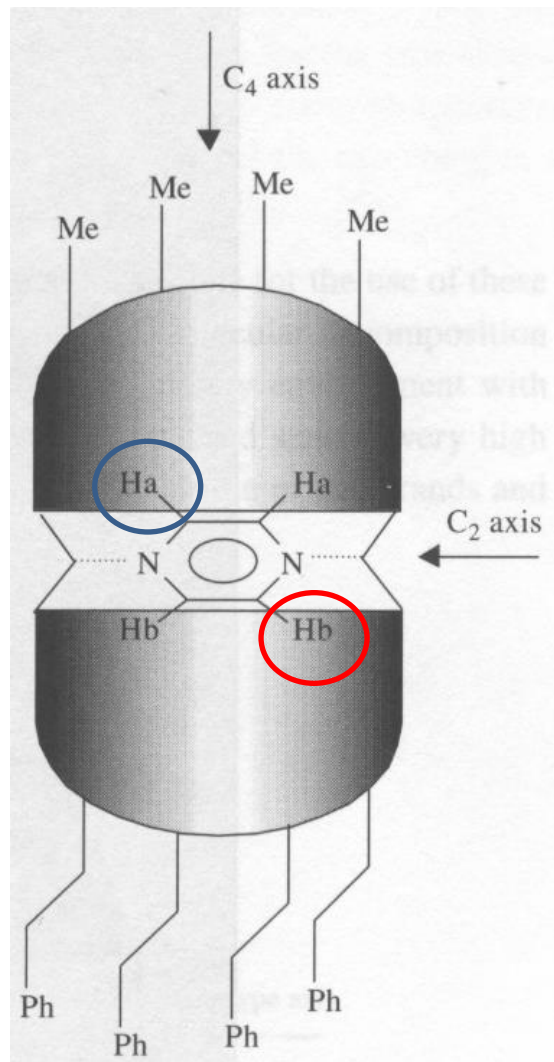
11•Guest $n = 2$ $R = \text{CH}_2\text{CH}_2\text{Ph}$

12•Guest $n = 3$ or $\text{C}_{11}\text{H}_{23}$



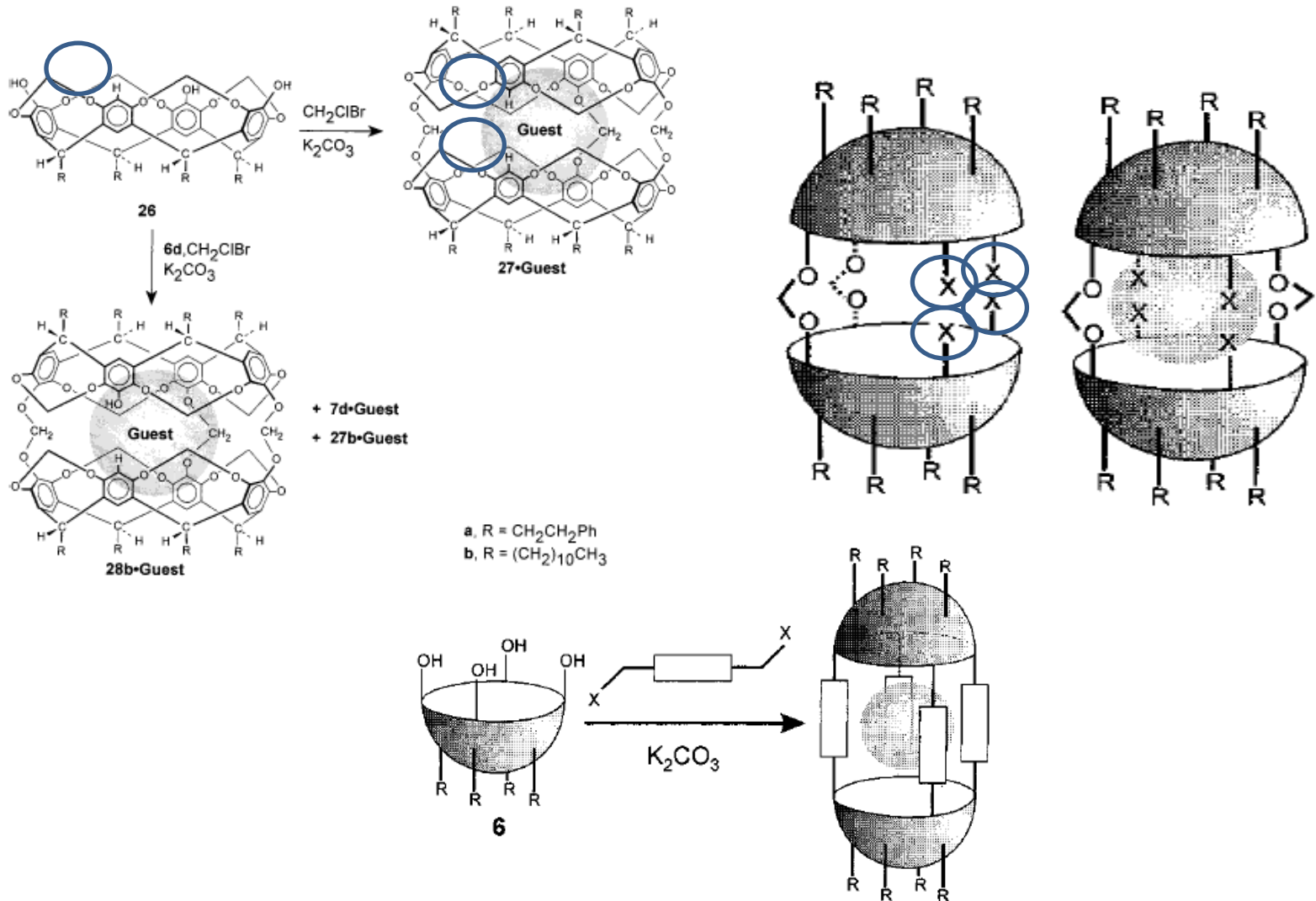
13•Guest $R = (\text{CH}_2)_4\text{CH}_3$

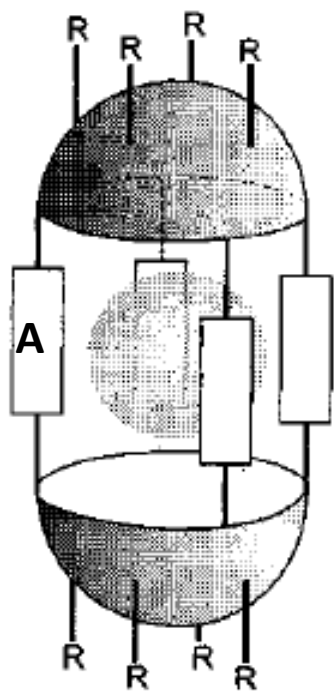




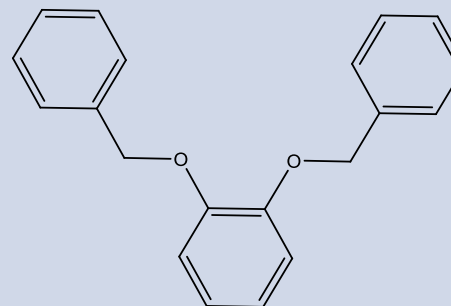
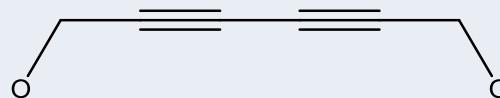
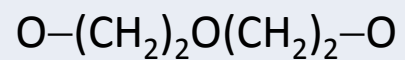
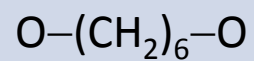
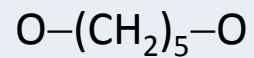
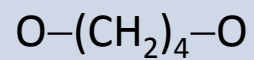
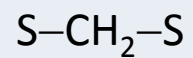
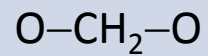
Emicarcerando:

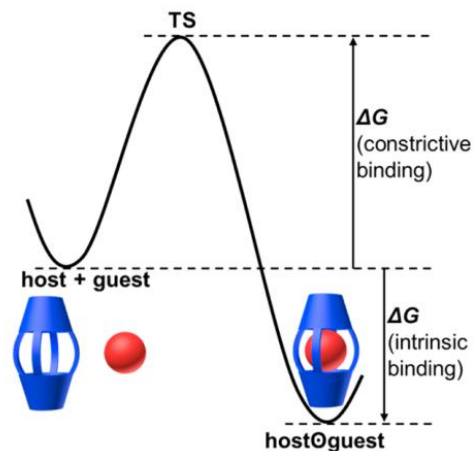
Contenitore molecolare chiuso (capsula) che definisce cavità sferica, i guest sono intrappolati (all'atto della sintesi) - entrata e uscita senza rottura di legame covalente, i.e. velocità di scambio misurabile





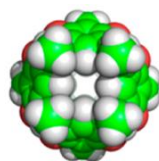
A



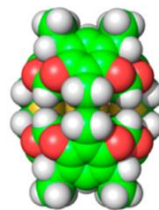


Intrinsic binding, the free energy of complexation, depends on the magnitude of the noncovalent interactions between the guest and the host's inner surface.

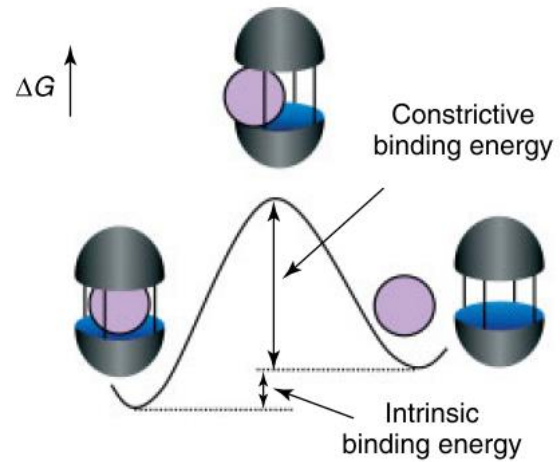
Constrictive binding, activation energy required for a guest to enter the inner cavity of a hemicarcerand through a size restricting portal in the host's skin.



top-view

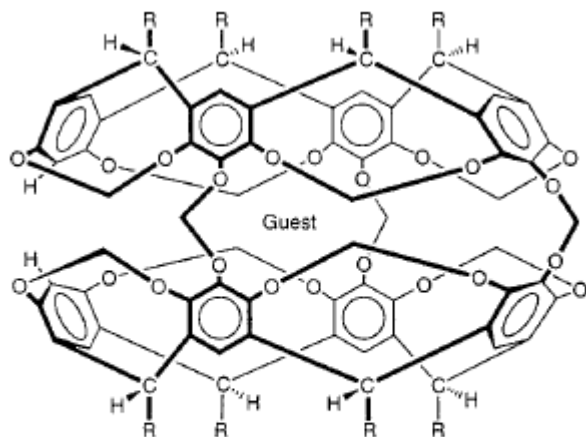


side-view

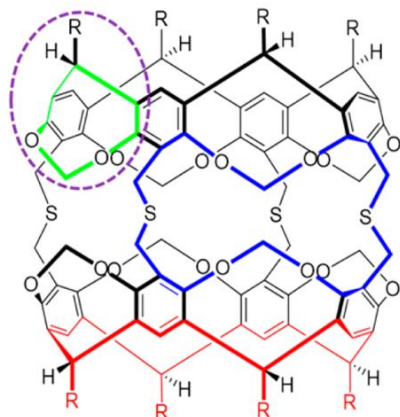
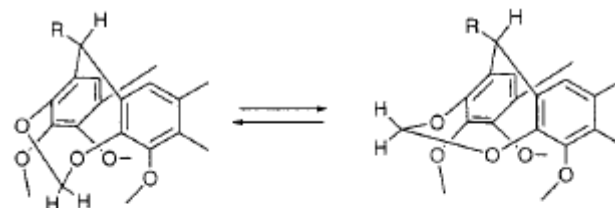


Constrictive binding: aumenta con le dimensioni del guest, diminuisce con le dimensioni dei portali, e con l'aumento della flessibilità dei linker (T).

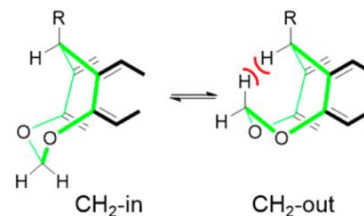
Gate mechanisms (molecular mechanics calculations) – **French door**
 chair-to-boat transition of the methylene bridges, calculated barrier 22 kcal/mol.



12 ⊕ Guest
 R = CH₂CH₂Ph

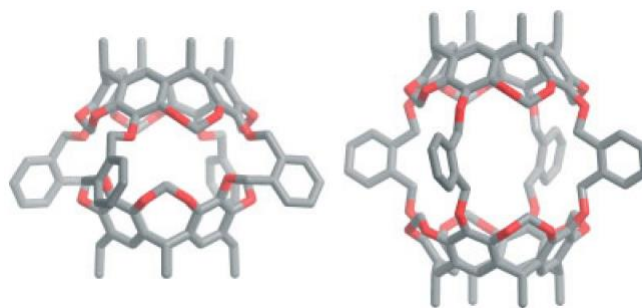
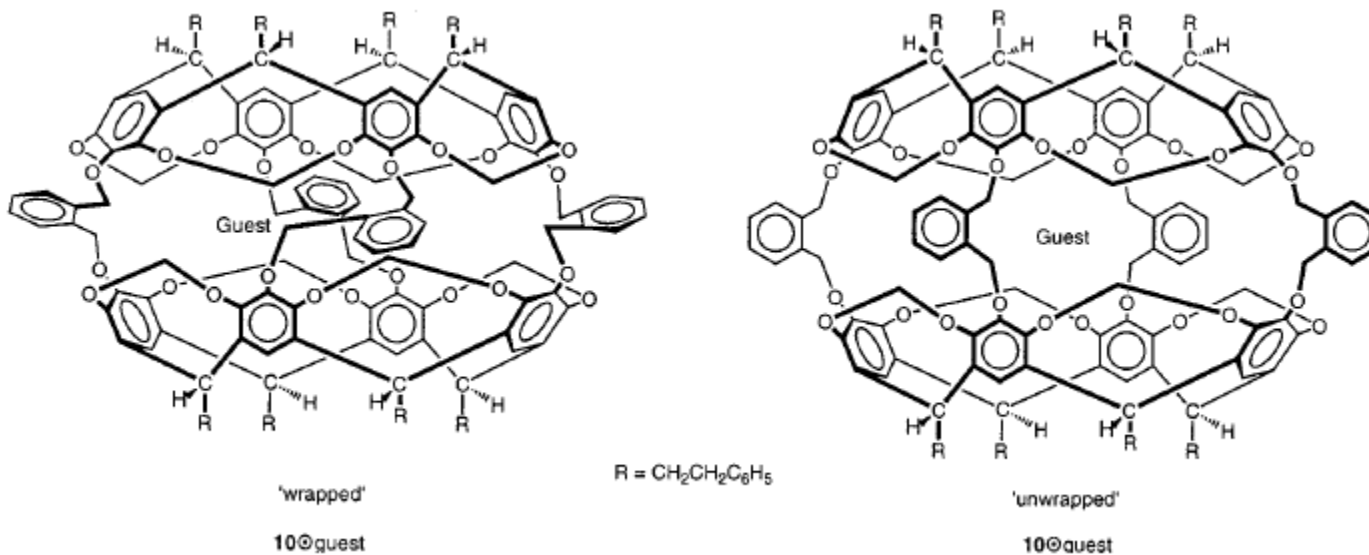


1a. R = (CH₂)₂Ph
 1b. R = Me

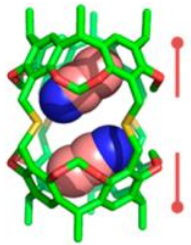
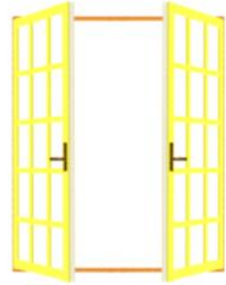
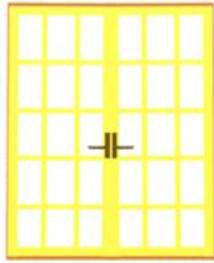


Gate mechanisms (molecular mechanics calculations) – **Sliding door**

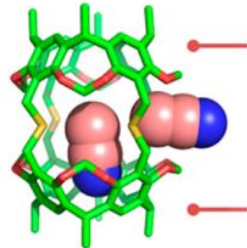
twisting and untwisting of the two host cavitands – measured barrier (VT NMR) 12.6 kcal/mol



a. French door

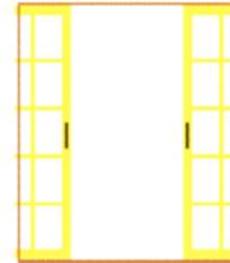
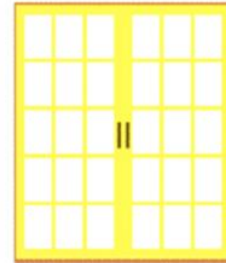


closed



open

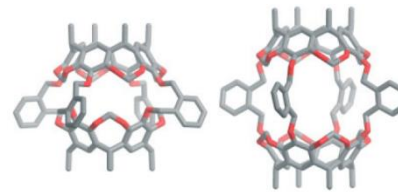
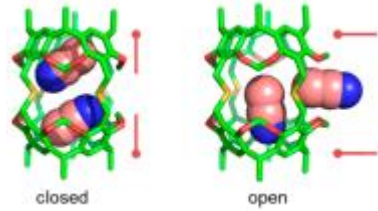
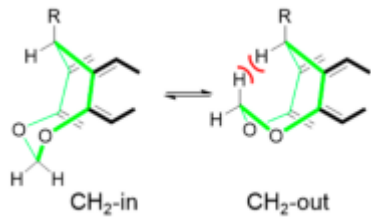
b. Sliding door

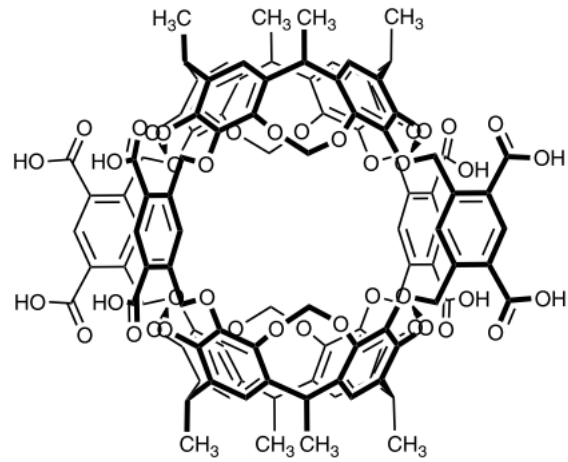


closed



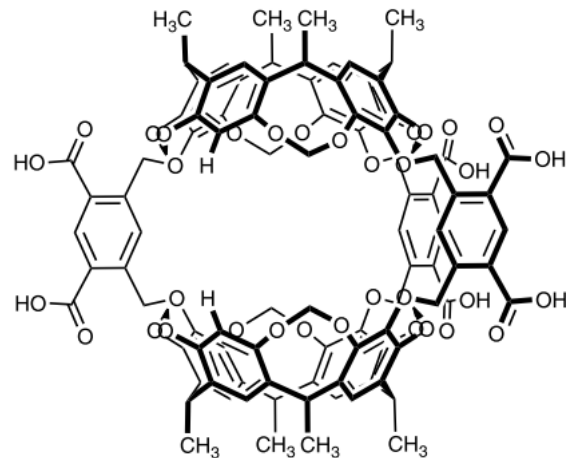
open



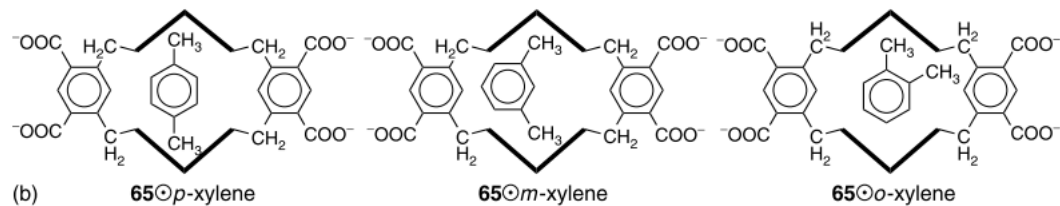


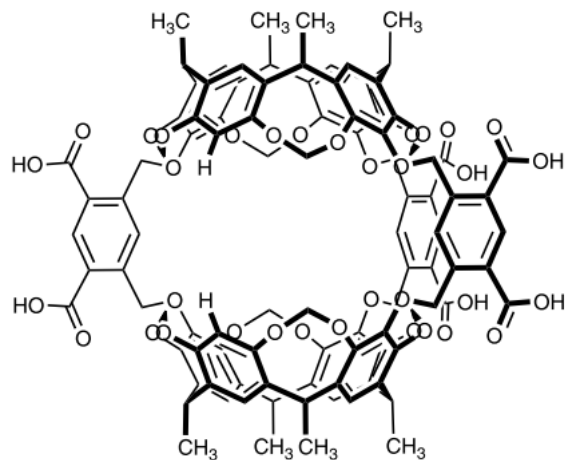
Water soluble octa-acid hemicarcerand:

Hydrophobic effect (higher than cyclodextrines)!

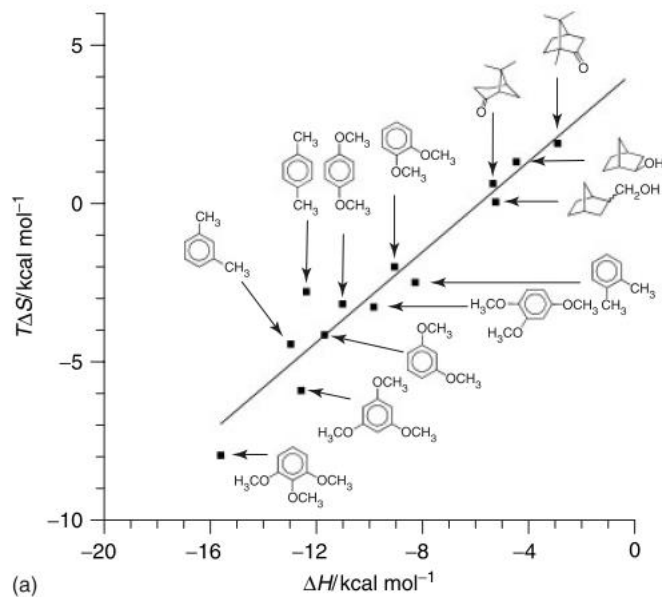


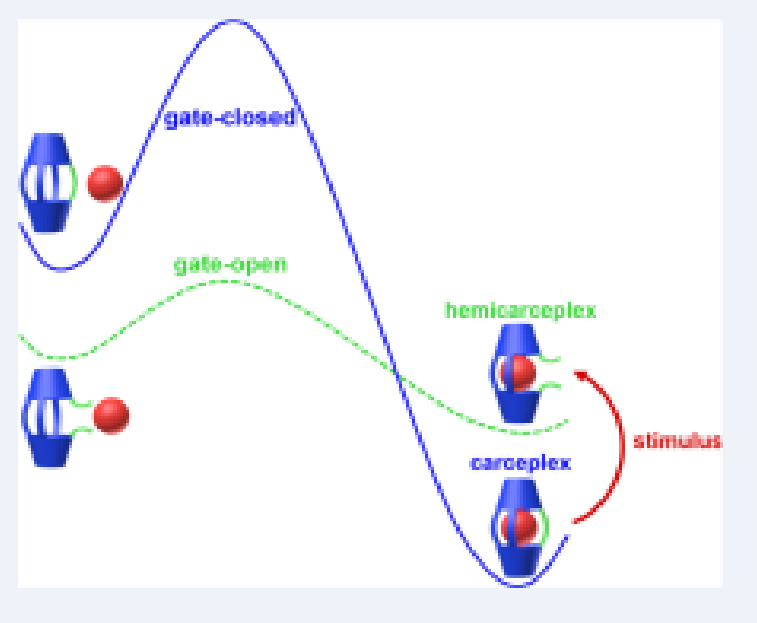
CH- π interactions for isomeric xylenes or dimethoxybenzenes direct the order of affinity:
meta > para >> ortho





CH- π interactions for isomeric xylenes or dimethoxybenzenes direct the order of affinity:
meta > para >> ortho

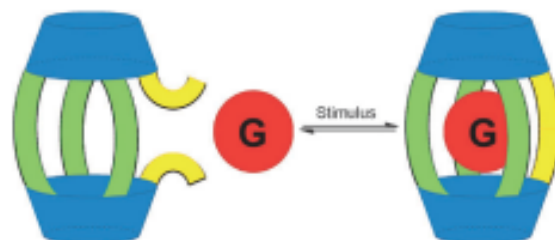


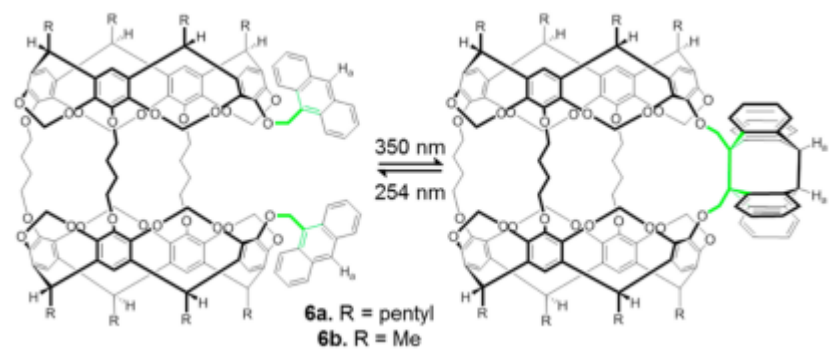
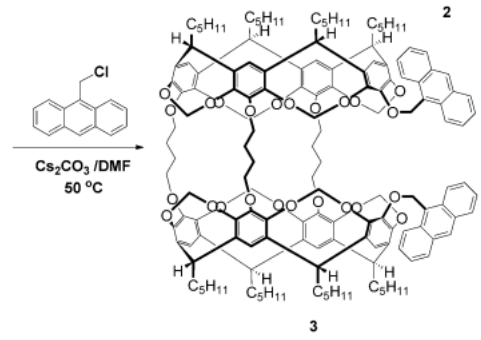
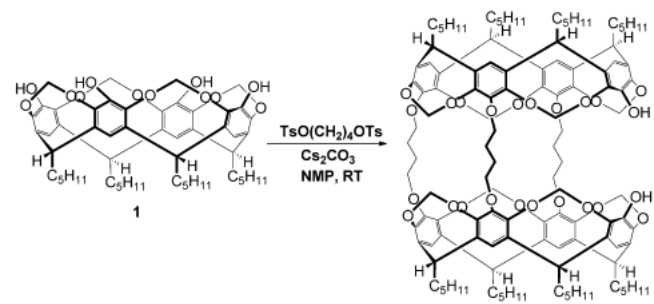


Reversible Photochemically Gated Transformation of a Hemicarcerand to a Carcerand**

Hao Wang, Fang Liu, Roger C. Helgeson, and Kendall N. Houk*

Angew. Chem. Int. Ed. 2013, 52, 655–659





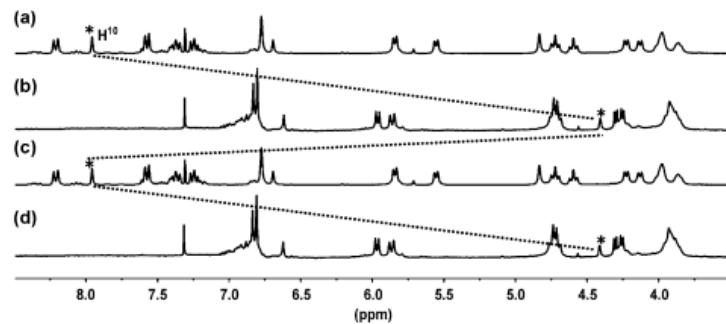
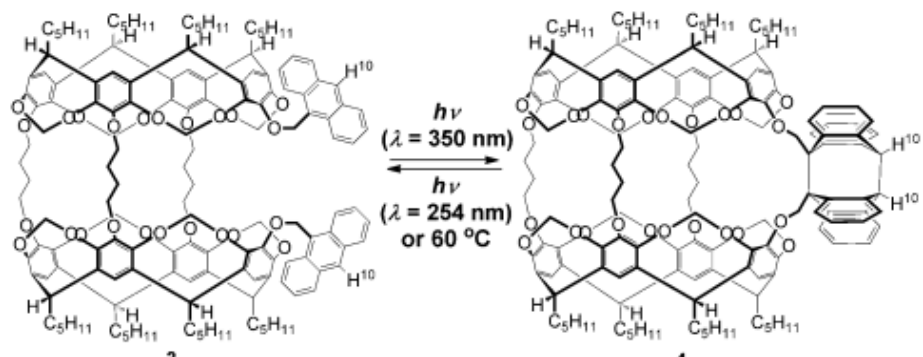
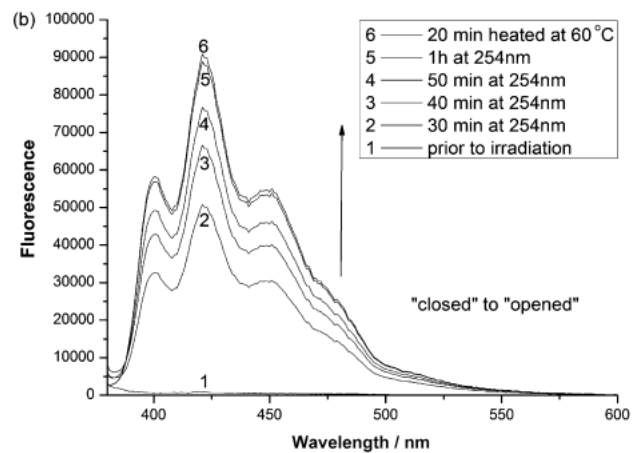
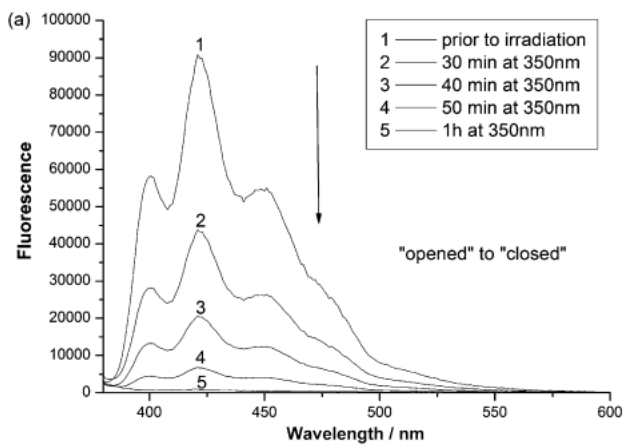
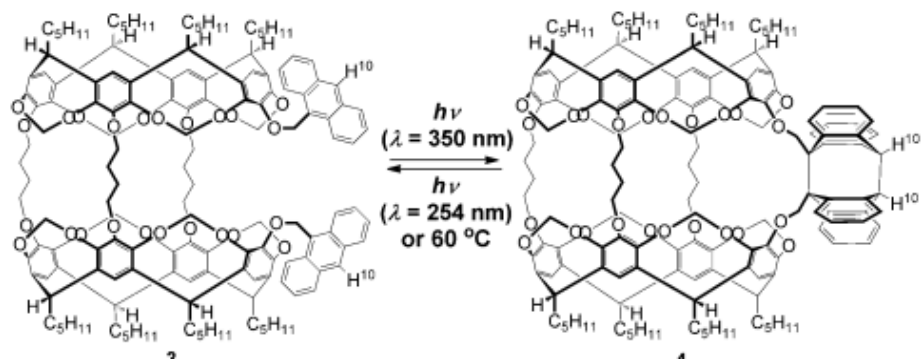
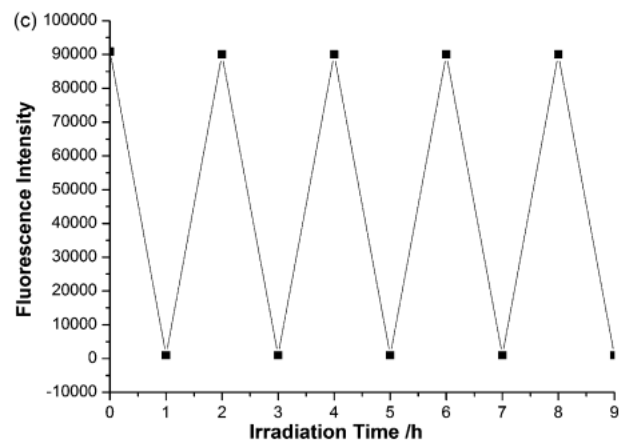
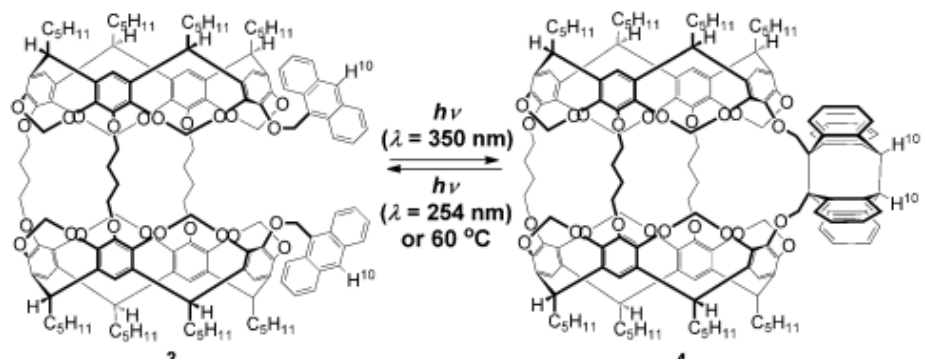
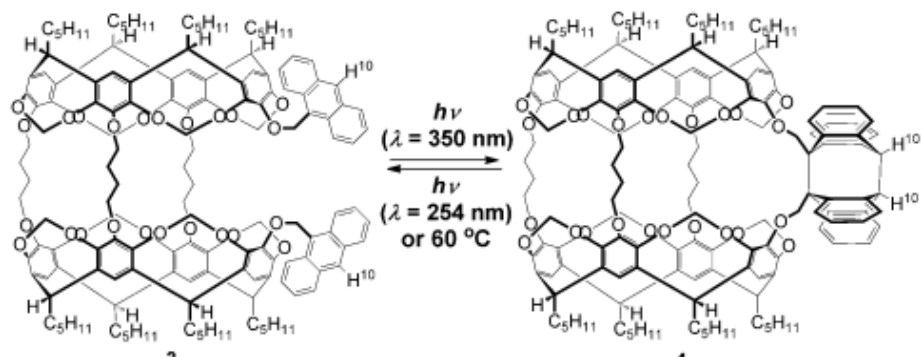


Figure 3. Partial ^1H NMR spectra (400 MHz, CDCl_3) of a) host **3** b) irradiation of host **3** with light at 350 nm for 1 h, c) irradiation of b with light at 254 nm for 1 h or heating at 60°C for 20 min, d) irradiation of c with light at 350 nm for 1 h.







The progress of the photodimerization was also monitored by thin-layer chromatography, which showed only one band after completion of the photodimerization. Photodimer 4 was purified after photolysis at 350 nm. In the high-resolution mass spectrum the molecular ion of photoproduct 4 has the same mass as the parent open-state host 3.

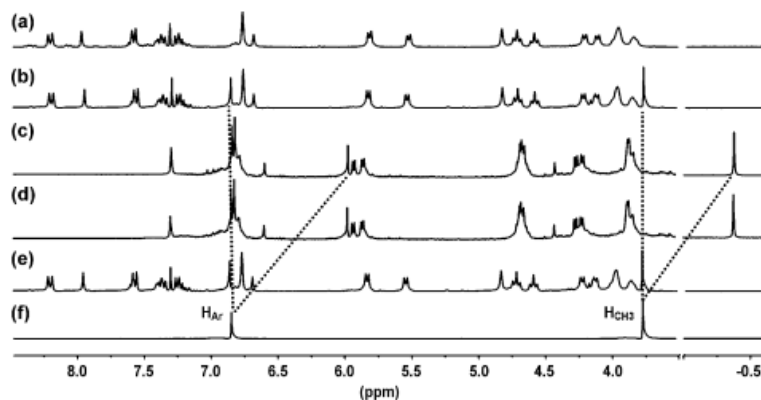
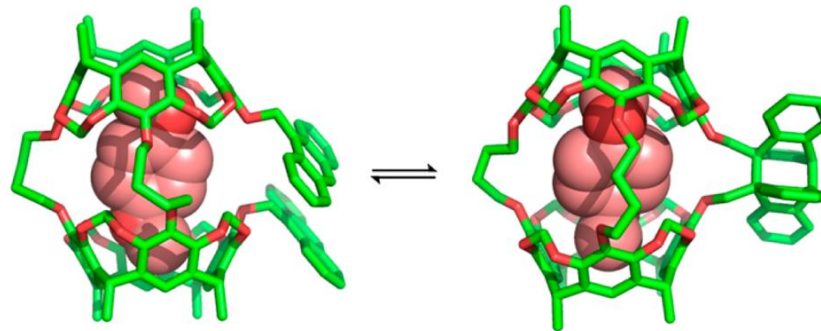
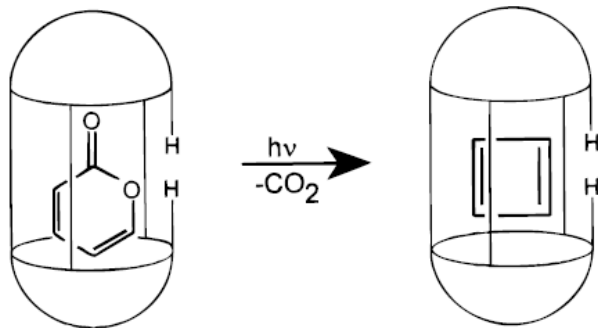


Figure 6. Partial ^1H NMR spectra (400 MHz, CDCl_3) of a) host **3** b) addition of 1 equiv of 1,4- $(\text{MeO})_2\text{C}_6\text{H}_4$ into host **3** solution without irradiation, c) **4** + 1,4- $(\text{MeO})_2\text{C}_6\text{H}_4$,^[16] d) c after 4 weeks in dark and RT, e) irradiation of c with light at 254 nm for 1 h or heating at 60°C for 20 min, f) guest 1,4- $(\text{MeO})_2\text{C}_6\text{H}_4$.

The Ph_2O mixture was irradiated at 350 nm for 1 h and then poured into 10 mL of MeOH. The precipitate was dissolved in CDCl_3 and the ^1H NMR spectrum was recorded (F. 6c). The methyl signal of the guest showed a shift from 3.78 to 0.37 ppm ($\Delta\delta = 4.15$ ppm), and the anthracene peaks of **3** disappeared (F. 6c). This indicates that after the gate of **3** is closed, a carceplex is formed between the carcerand **4** and the guest. MALDI mass spectra indicate formation of this carceplex. The carceplex **4@G** can stay in the dark at ambient temperature more than 4 weeks without detectable release of the guest molecule (F. 6d). As a result, the activation energy for decomplexation in the open state **3@G** and the incarcerated guest can egress easily. The gate-opened hemicarcerand is then almost exclusively filled with the solvent CDCl_3 .



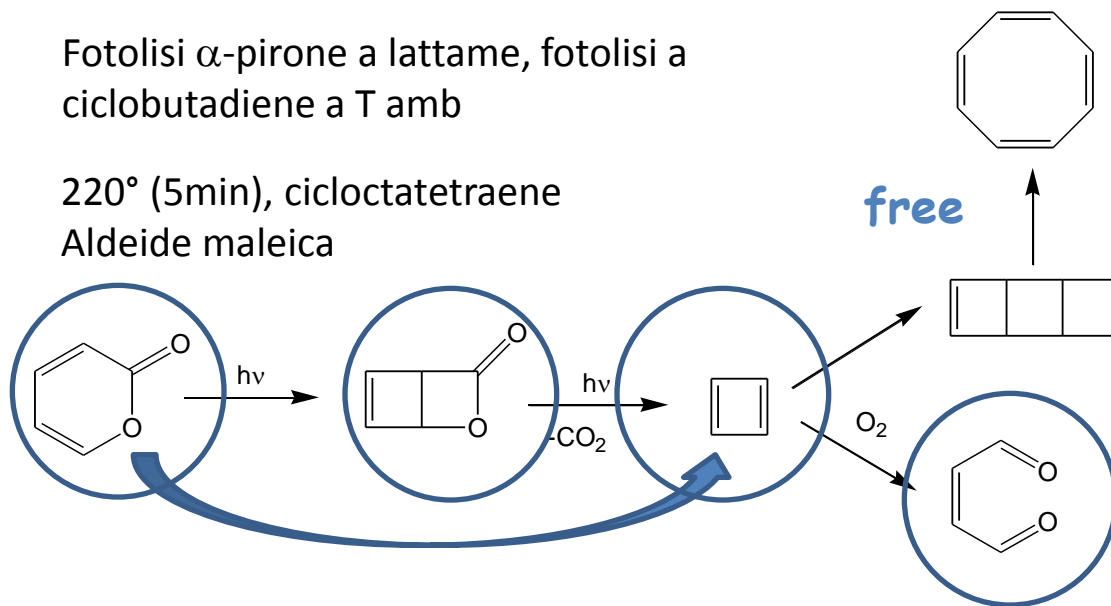
27a• α -pyrone

8K - matrice gas inerte congelato

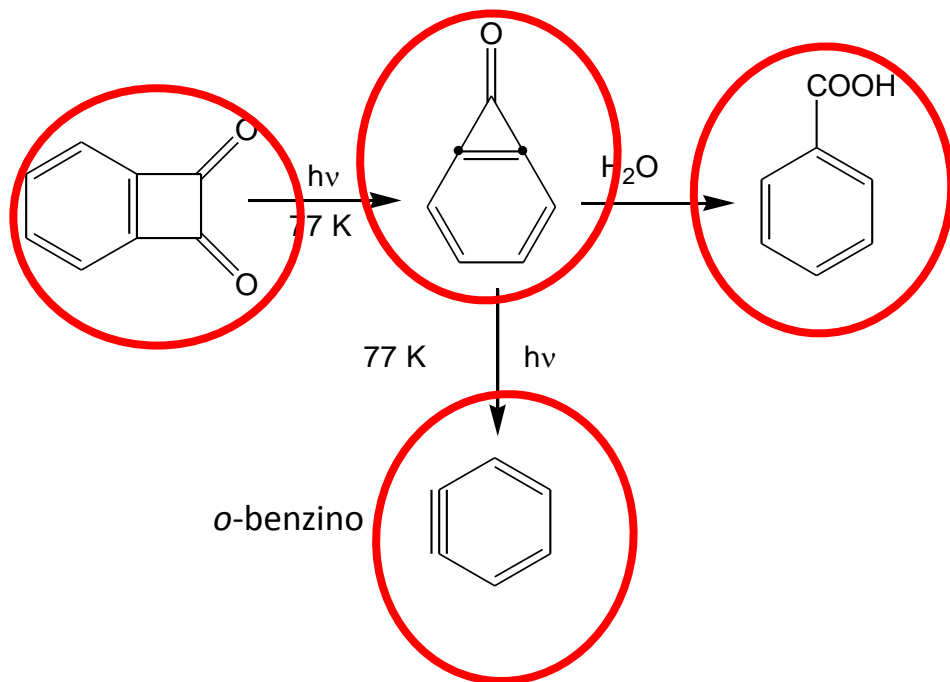
Fotolisi α -pirone a lattame, fotolisi a
ciclobutadiene a T amb

220° (5min), cicloctatetraene

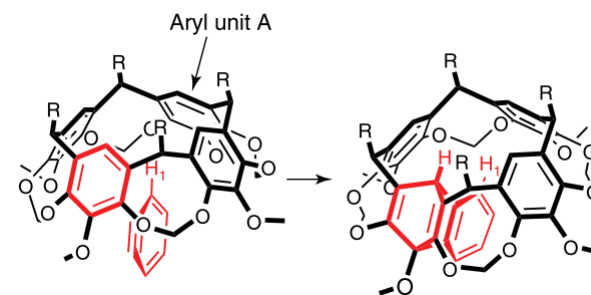
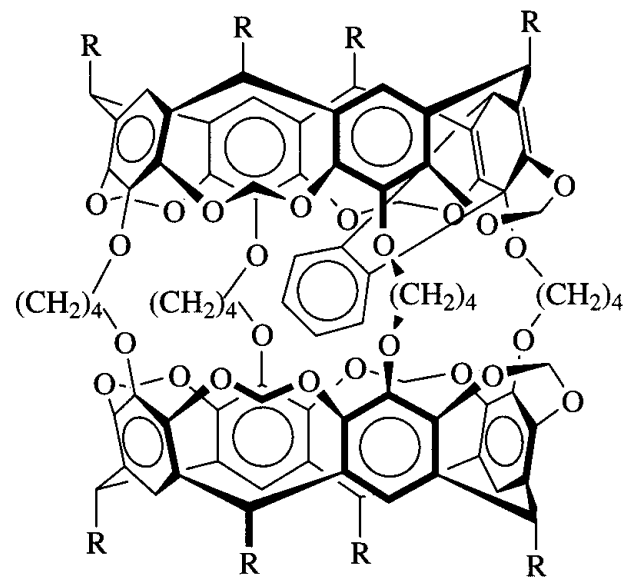
Aldeide maleica



Benzociclobutendione Benzociclopropenone



^1H e ^{13}C NMR a bassa T



First containers with the ability to permanently encapsulate a single molecule;
Strong contributions to what is perhaps the most exciting application of molecular containers:

use as molecular reaction flasks (or “nanoreactor”) in which otherwise fleeting species or labile intermediates can be generated and gain longevity at room temperature.

We anticipate future use of hemicaricplex in the following fields:

catalysis

drug and radiation delivery

release systems

separation science

guest-indicator systems,

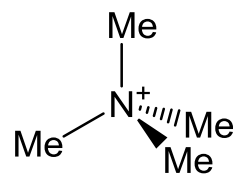
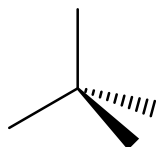
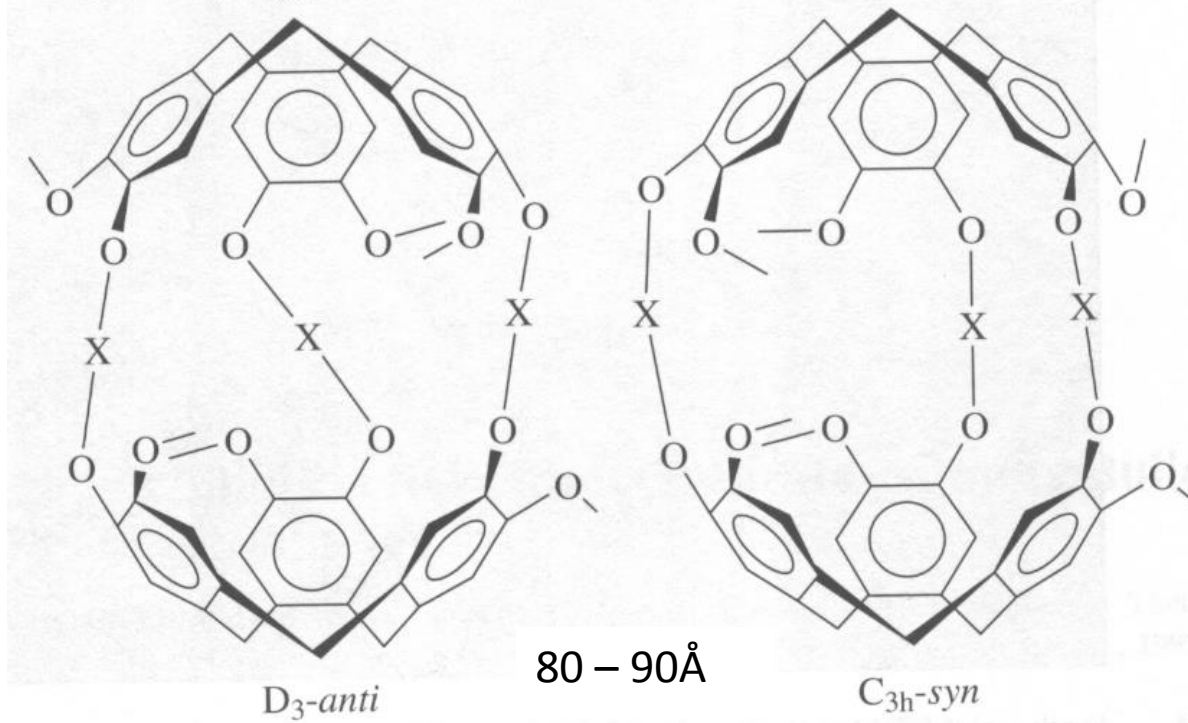
light-electrical switches

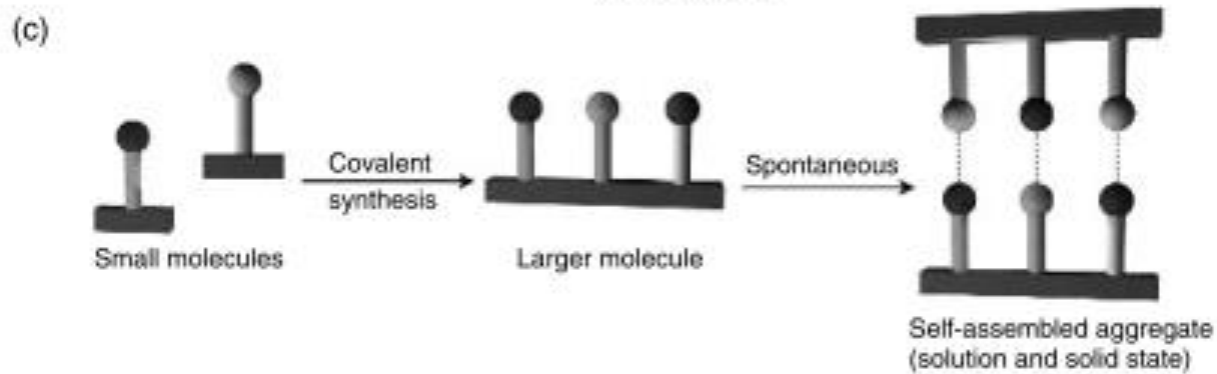
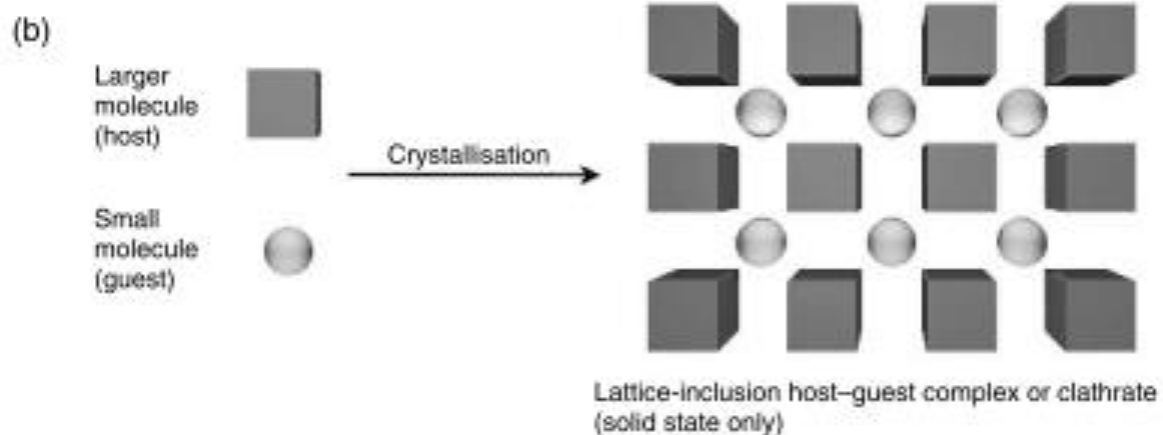
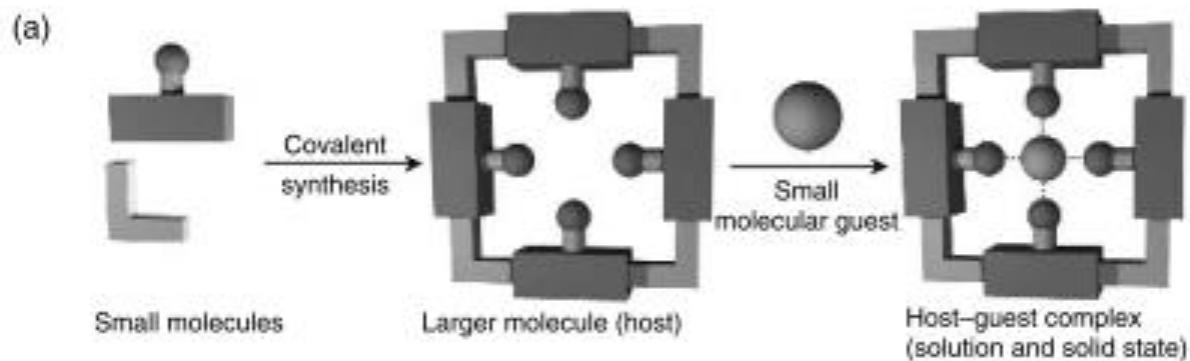
memory storage devices

scavenging impurities for water purification

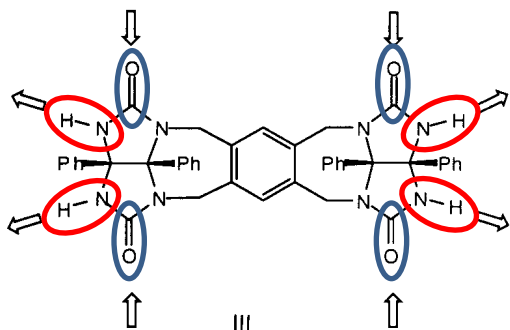
Criptofani

$X = \text{---}(\text{CH}_2)_n\text{---}, \text{---CH}_2\text{---CH=CH---CH}_2\text{---}, \text{alkyne}, \text{C}_6\text{H}_4$

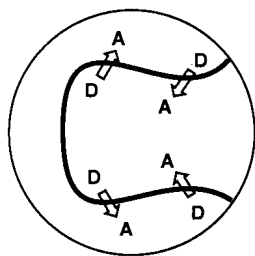




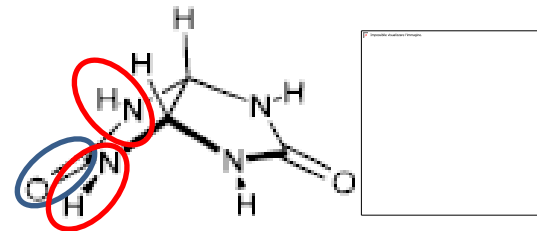
Tennis-ball



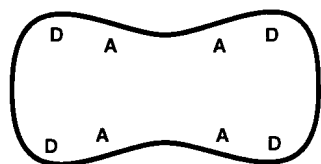
D = hydrogen bond donor
A = hydrogen bond acceptor



tennis ball

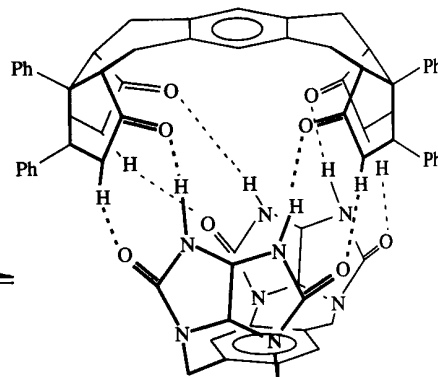
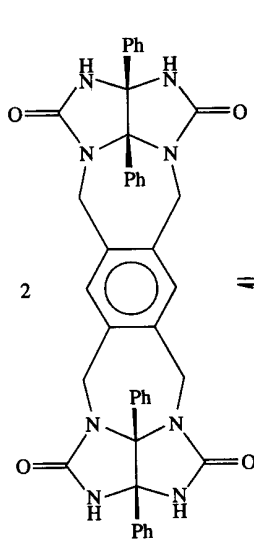


unità glicolurile

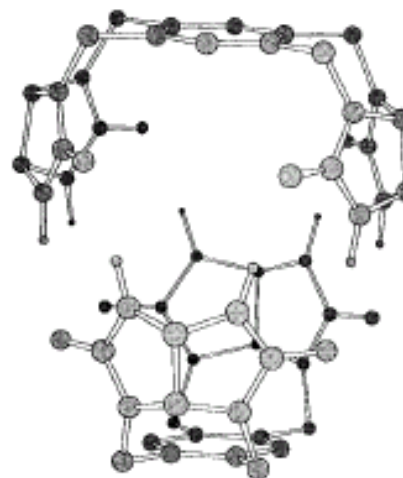


self-assembly

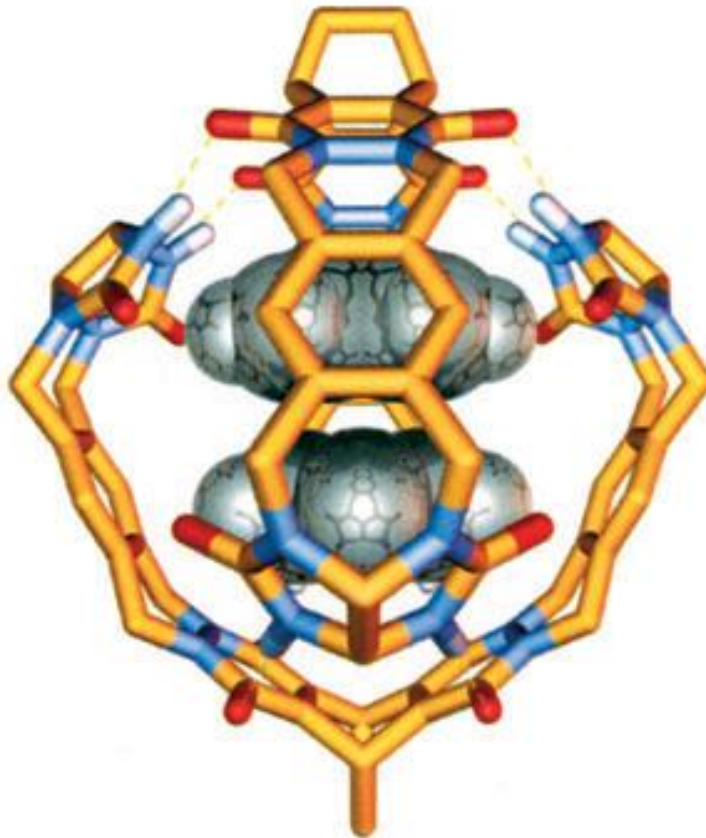
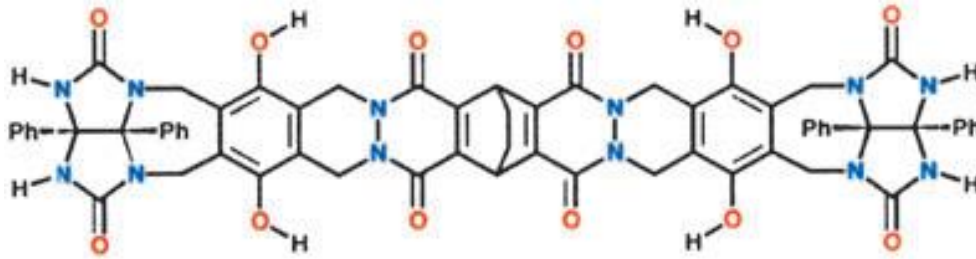
The formation of a molecular tennis ball



V ca. 60 \AA^3

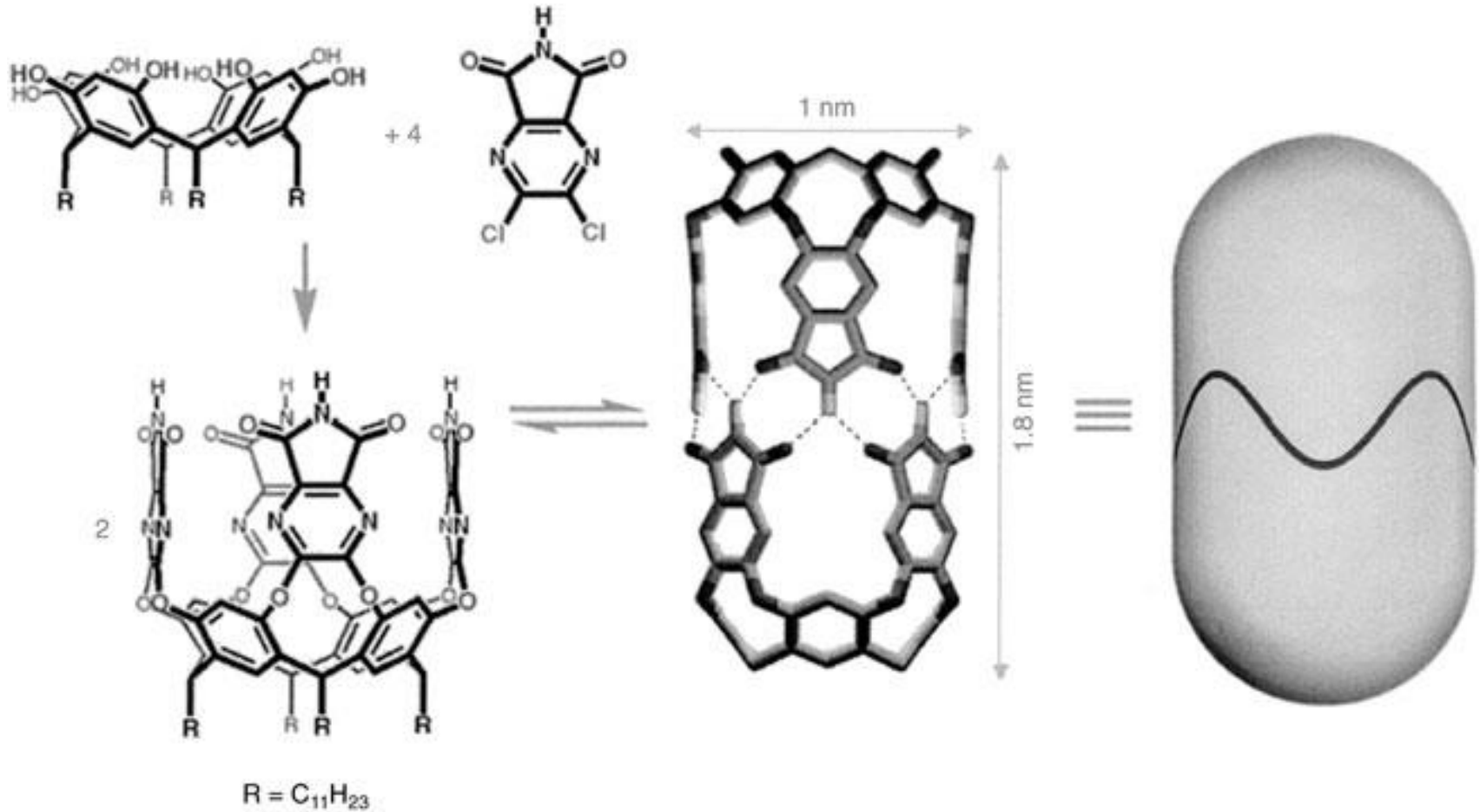


Soft-ball



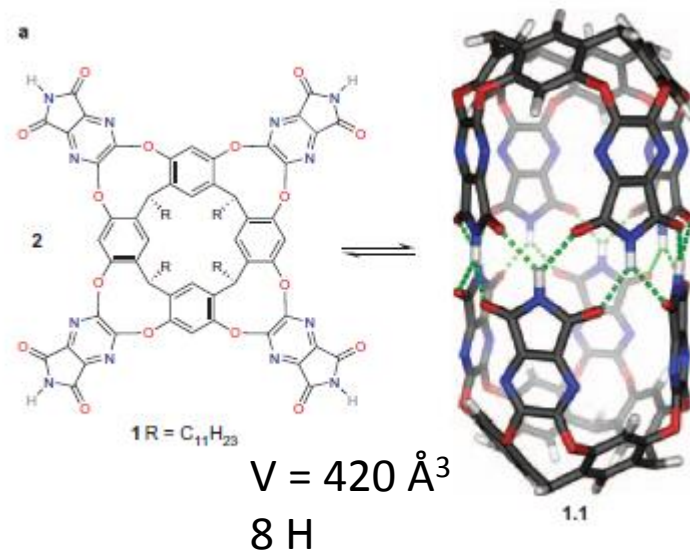
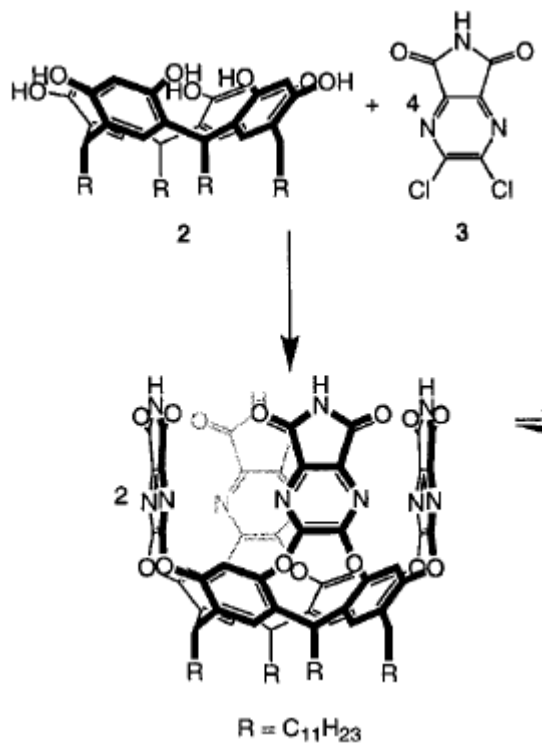
V ca. 400 Å³

Molecular Cylinder

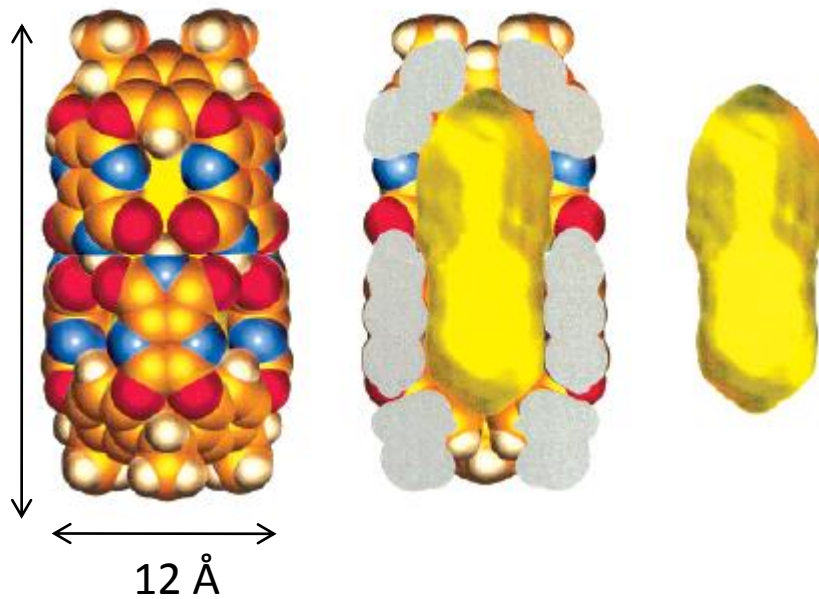


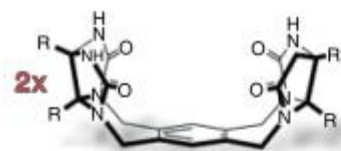
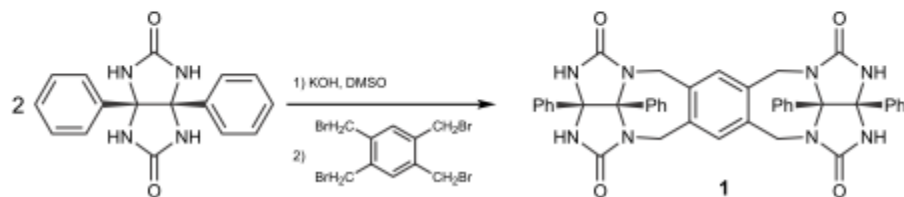
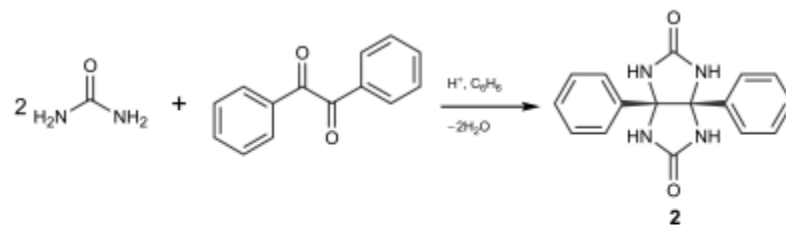
$V \text{ ca. } 420 \text{ \AA}^3$

Molecular Cylinder

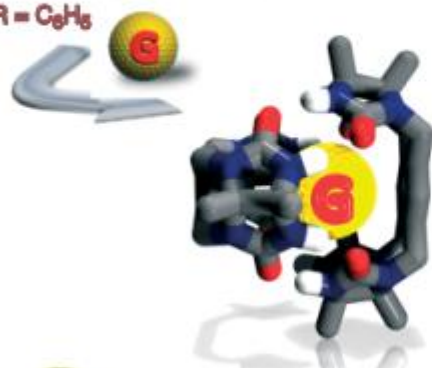


16 Å





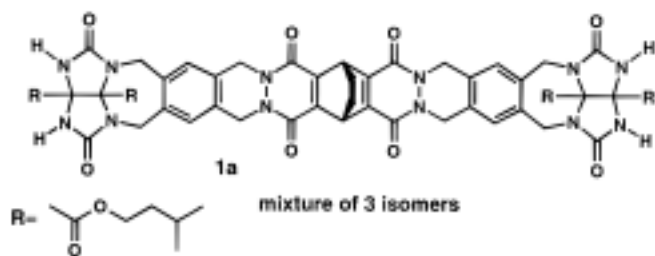
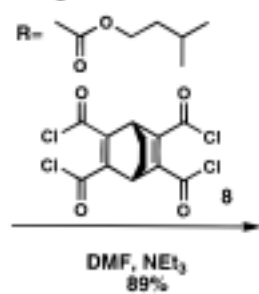
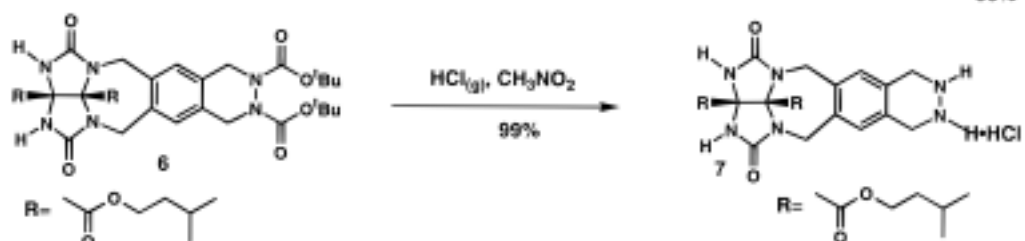
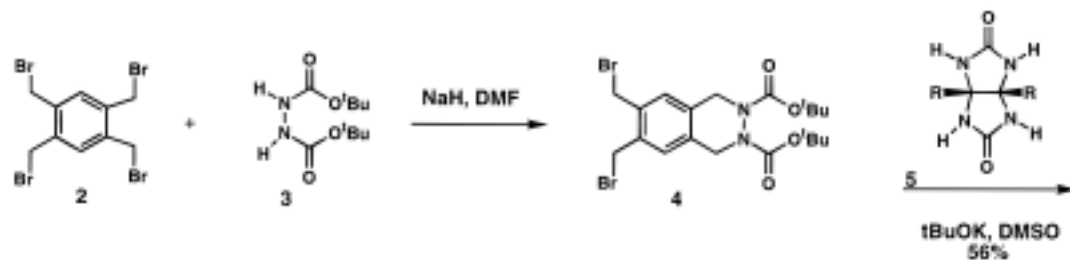
$\text{R} = \text{C}_6\text{H}_5$

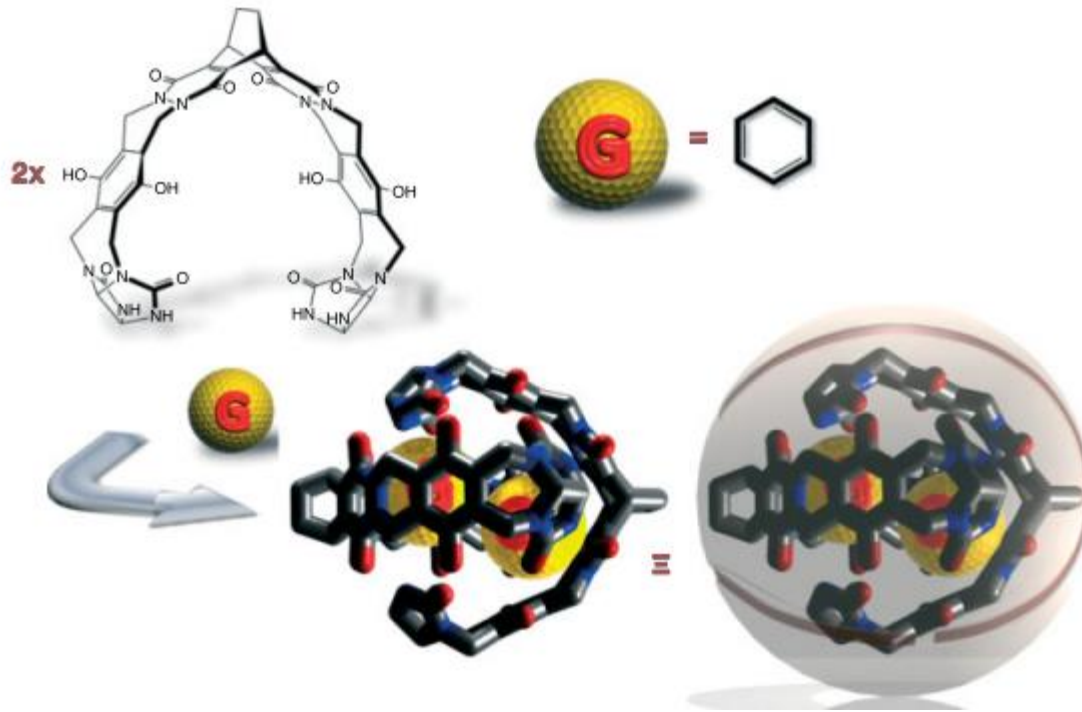


|||

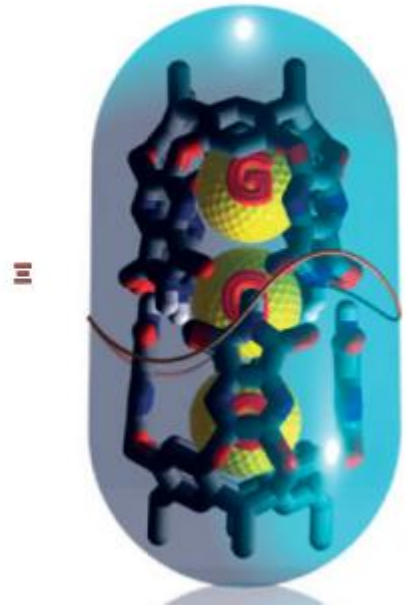
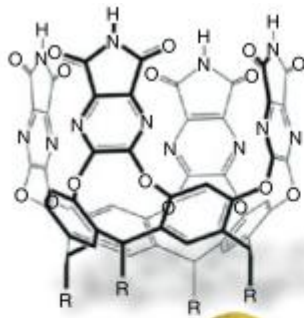
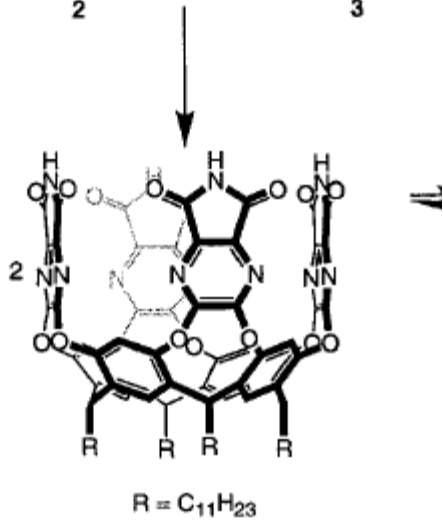
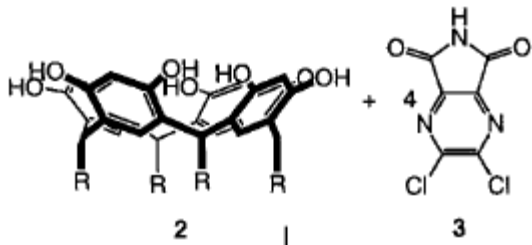


$V \text{ ca. } 60 \text{ \AA}^3$





V ca. 400 Å³

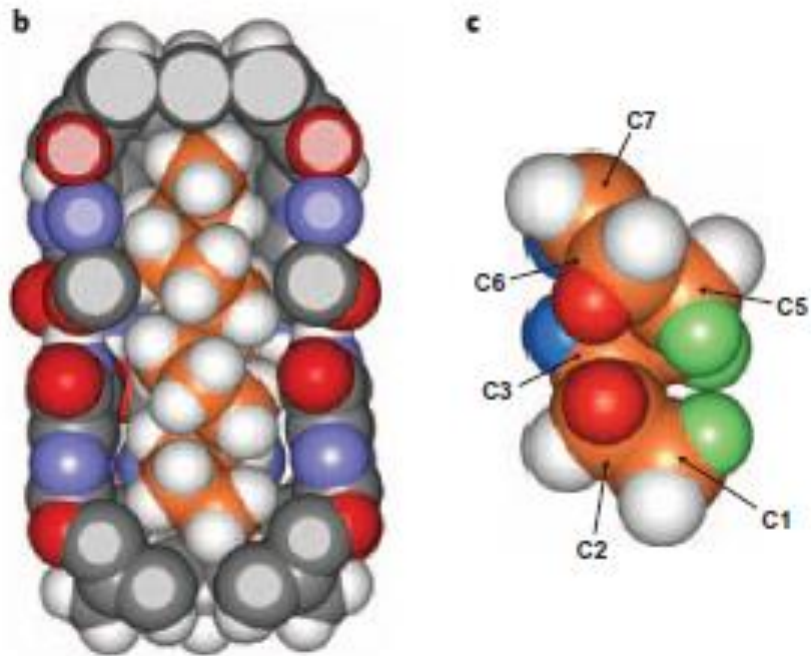


$V \text{ ca. } 420 \text{ \AA}^3$

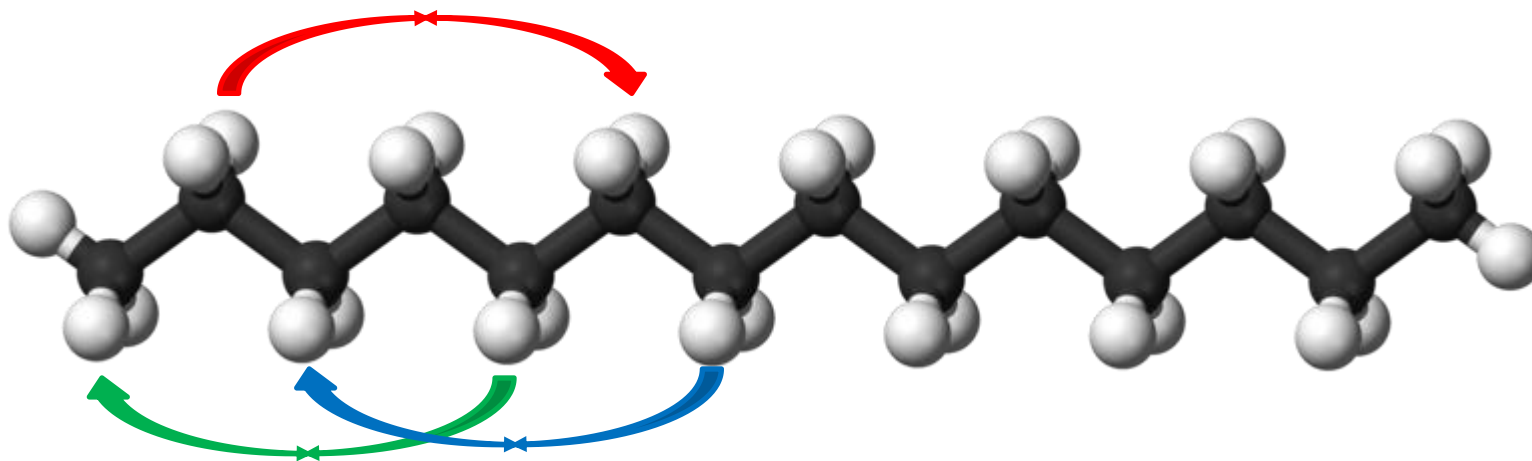
From molecular mechanics calculations:

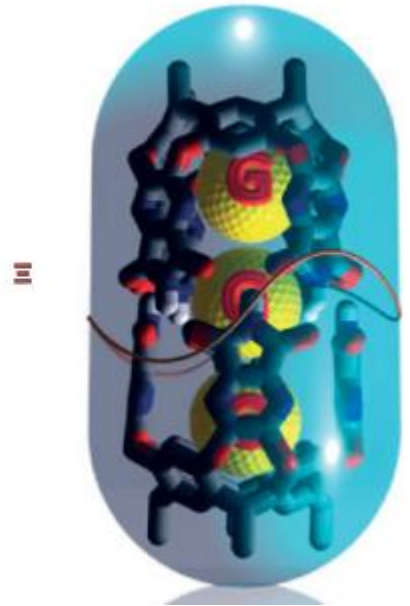
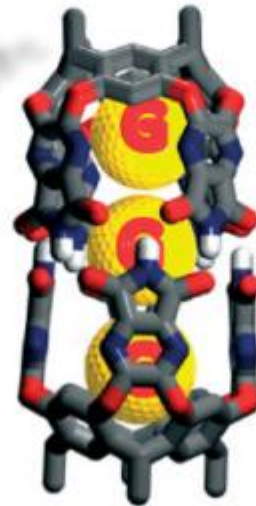
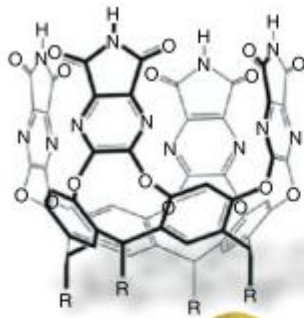
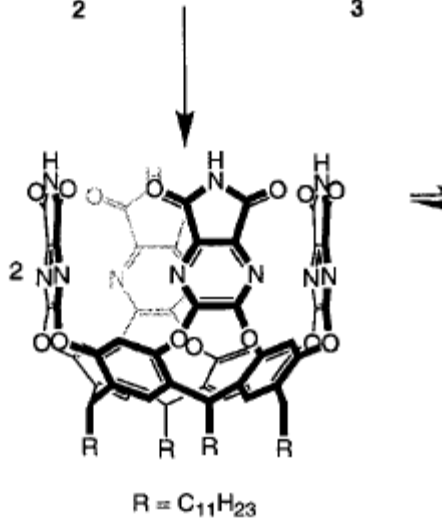
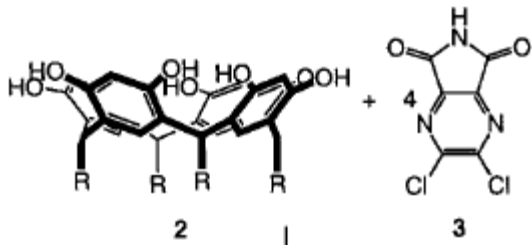
the encapsulated guest(s) occupy approximately 55% of the available space (same occupancy inside most weakly interacting organic solvents).

Stability decreases at higher or lower space occupancy.

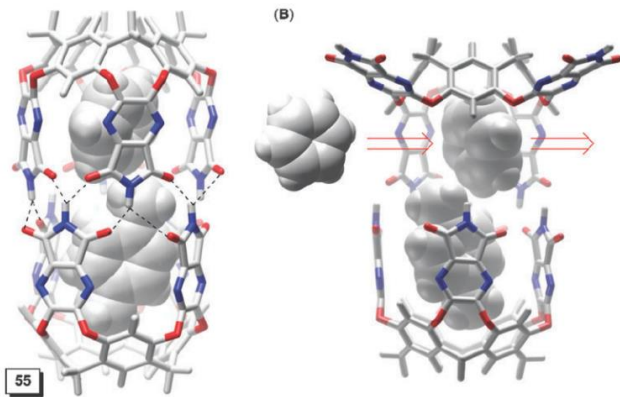
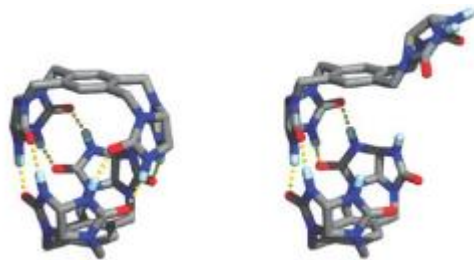


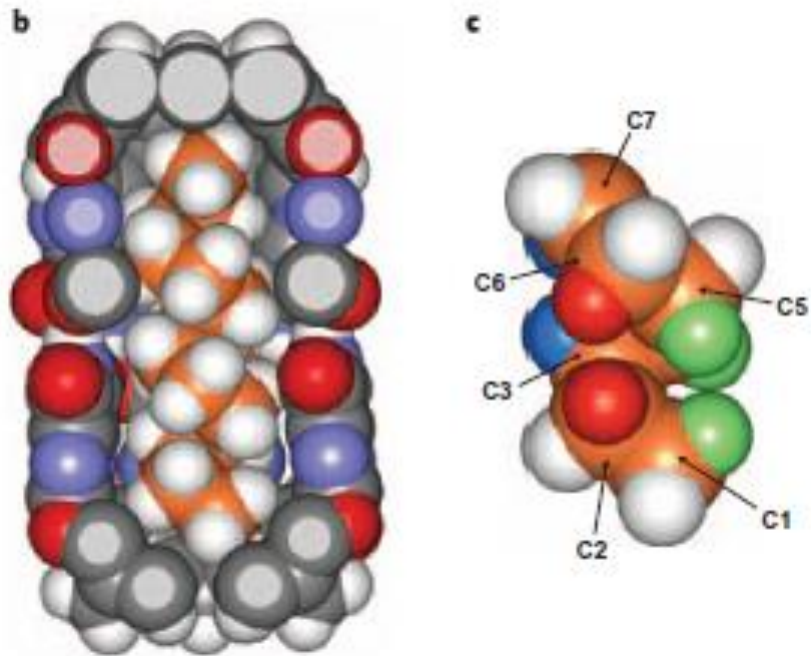
Model structure: incapsulation of coiled alkanes - tetradecane



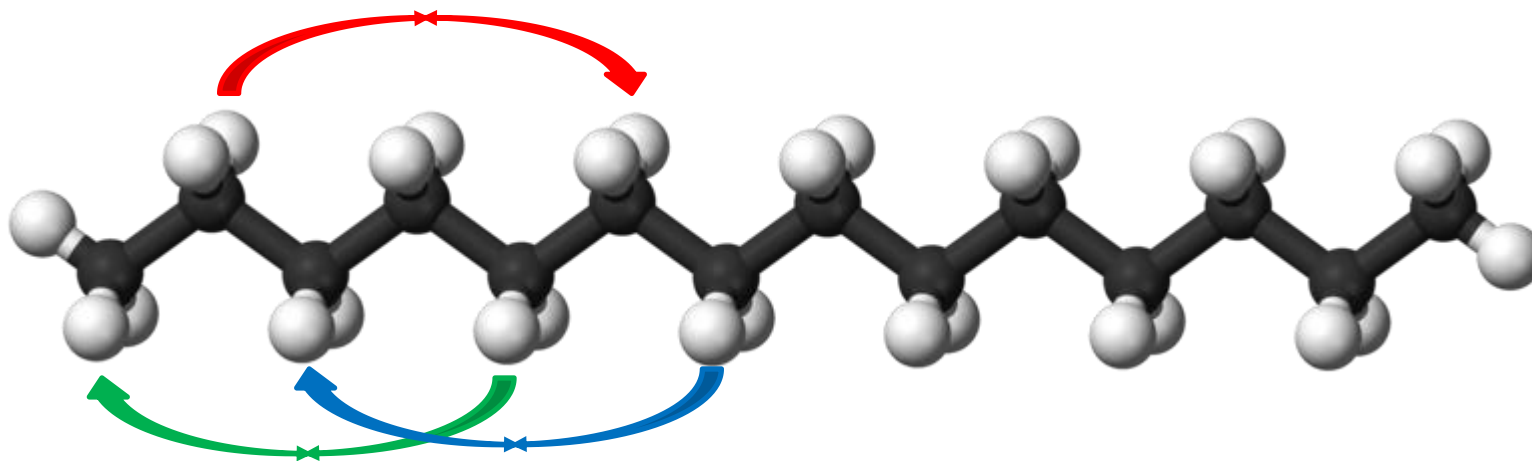


$V \text{ ca. } 420 \text{ \AA}^3$



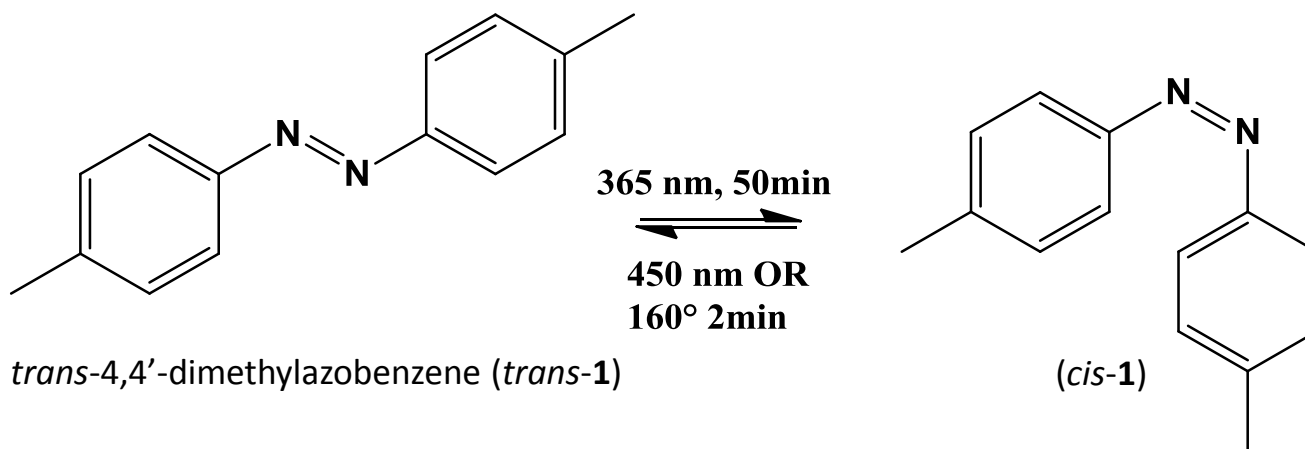


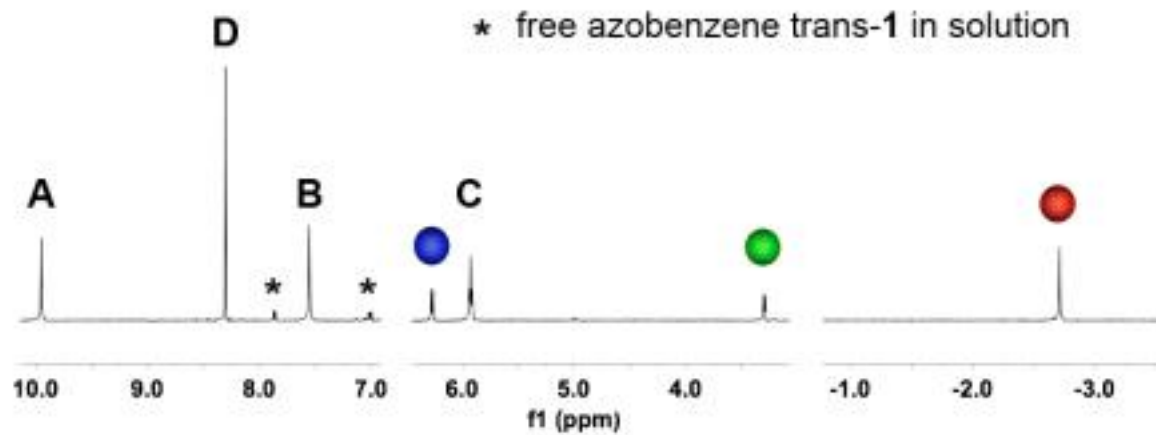
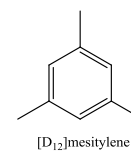
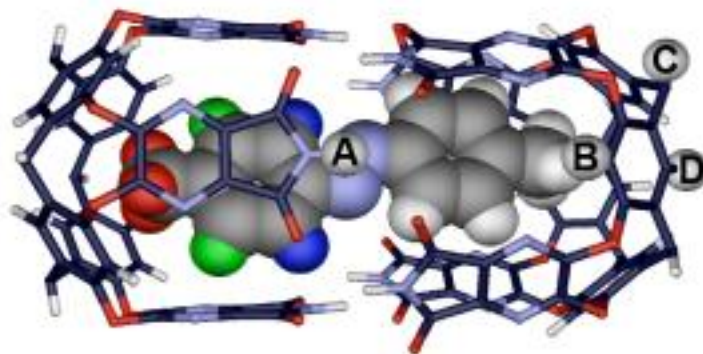
Model structure: incapsulation of coiled alkanes - tetradecane

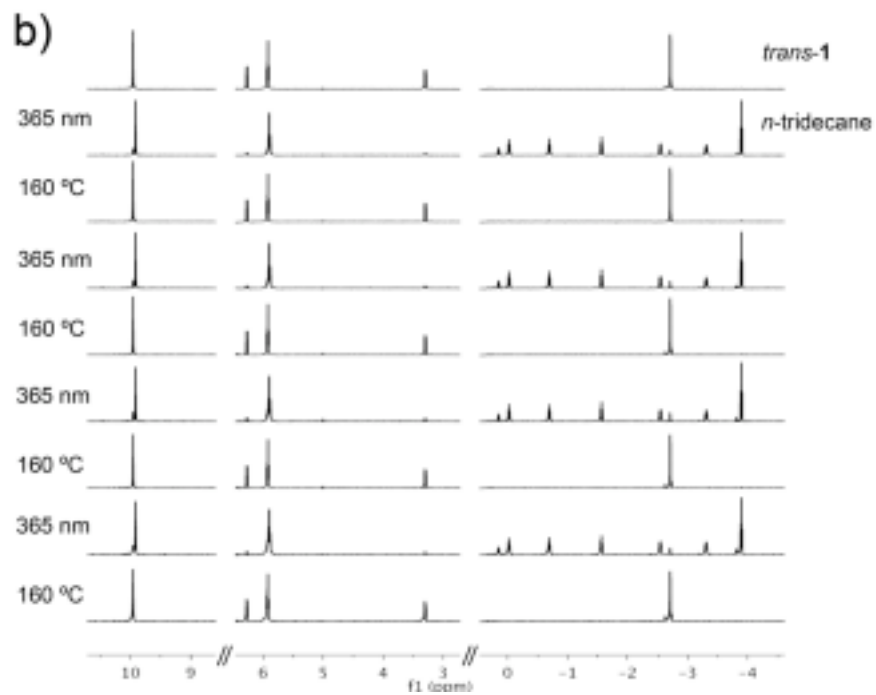
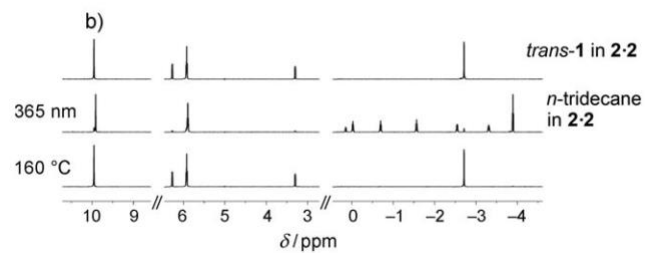
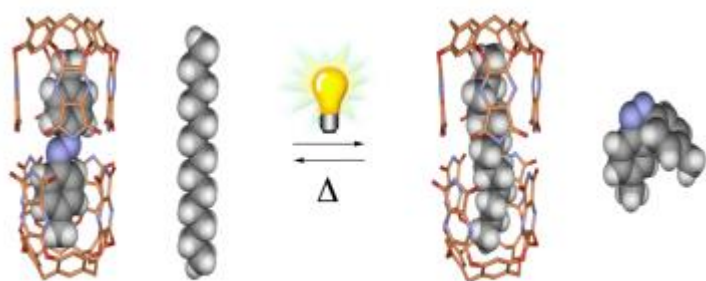
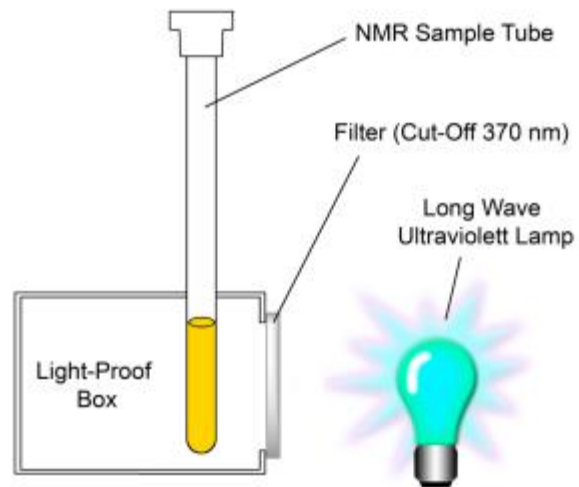


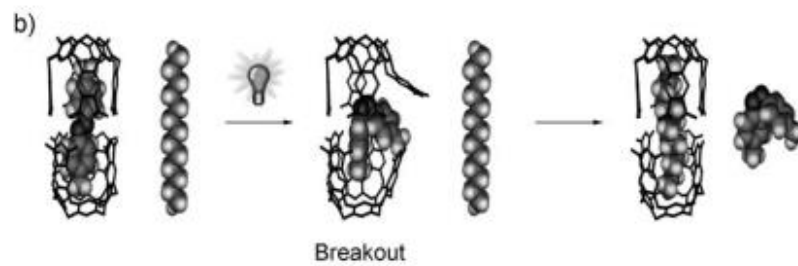
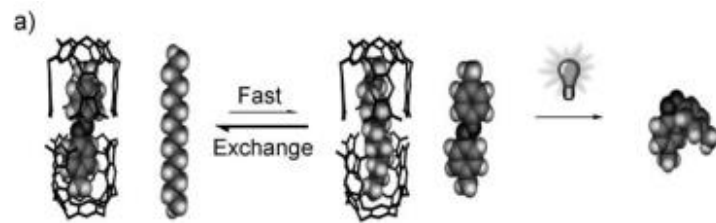
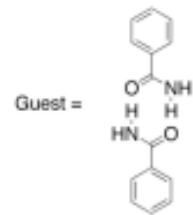
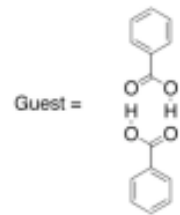
Photochemical Control of Reversible Encapsulation

Henry Dube, Dariush Ajami, and Julius Rebek, Jr.*



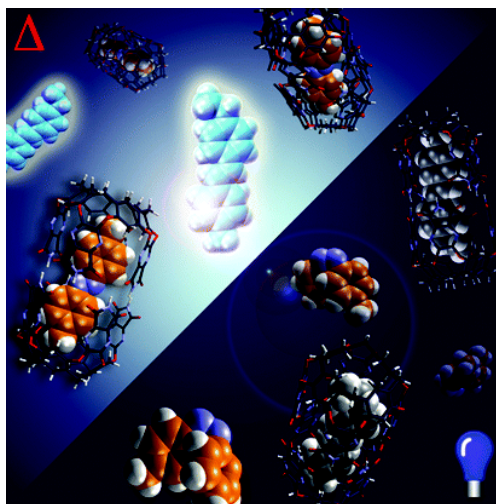
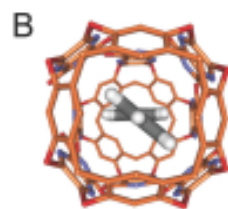
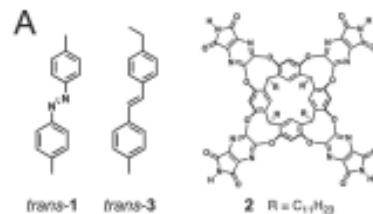






Supramolecular Control of Fluorescence through Reversible Encapsulation

Henry Dube,[‡] Mark R. Ams,[†] and Julius Rebek, Jr.*[‡]



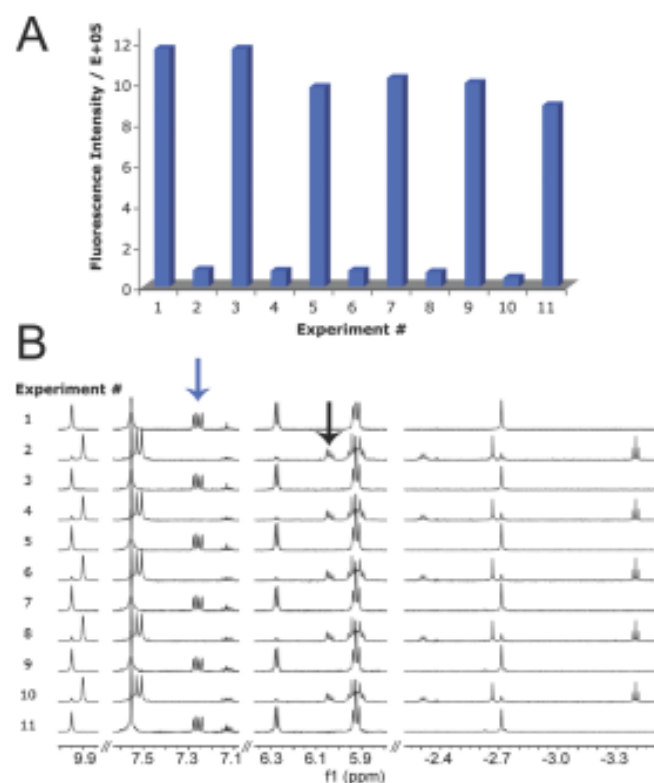
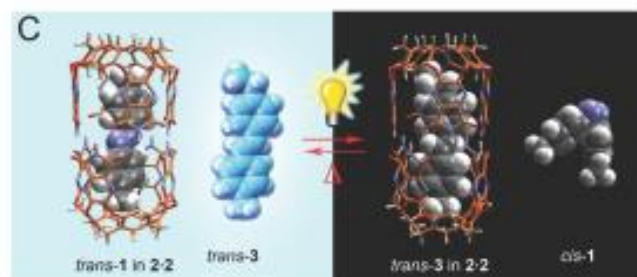


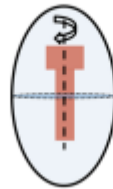
Figure 2. Reversible fluorescence intensity switching by light and heat. Five cycles of guest exchange and concomitant fluorescence change are shown. The numbers shown correspond to paired experiments for fluorescence measurement and ^1H NMR spectra. Odd experiment numbers indicate heating steps (160 °C for 2 min); even numbers indicate irradiation steps (365 nm for 50 min at 20 °C). (A) Fluorescence measured at 388 nm on excitation at 318 nm. (B) Corresponding ^1H NMR spectra for each step. The blue arrow indicates proton signals of free *trans*-**3** in solution; the black arrow indicates two aromatic proton signals of encapsulated *trans*-**3**.

(a)



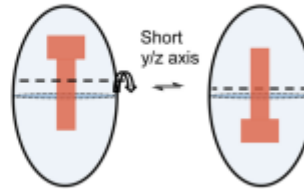
(b)

Long x-axis

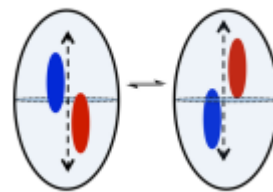


(c)

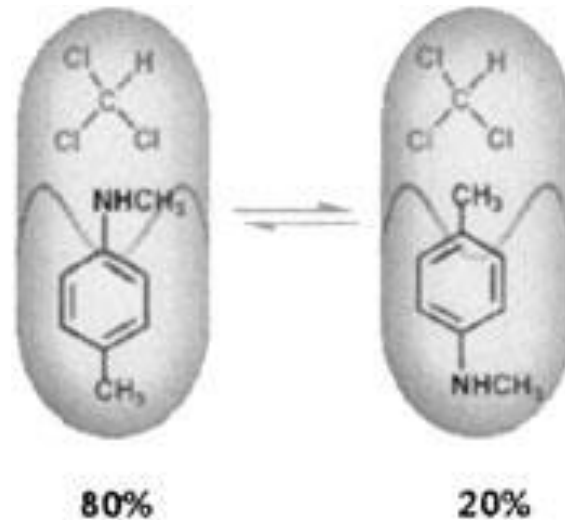
Short
y/z axis



(d)



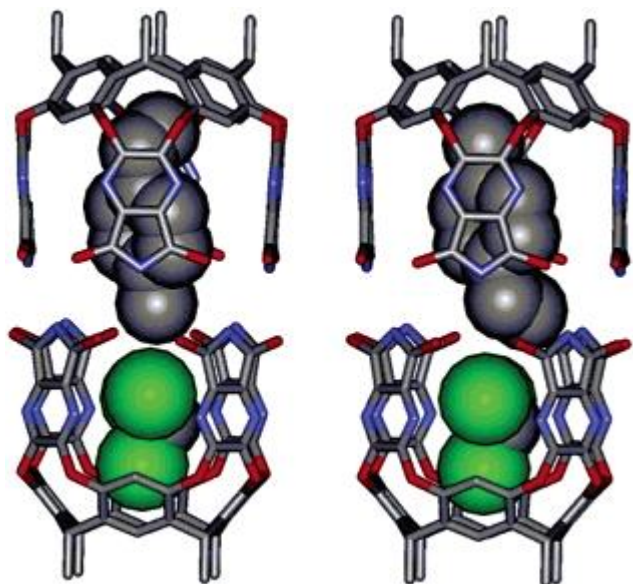
Social Isomers



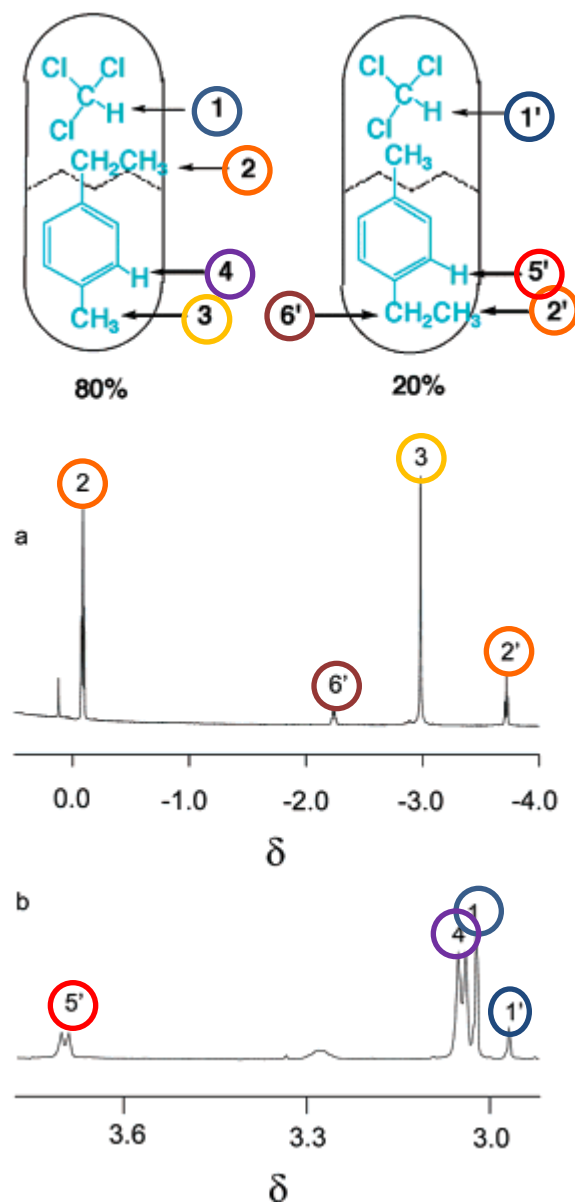
Cloroformio ed N-metil-*para*-toluidina, no interconversione

Social Isomers:

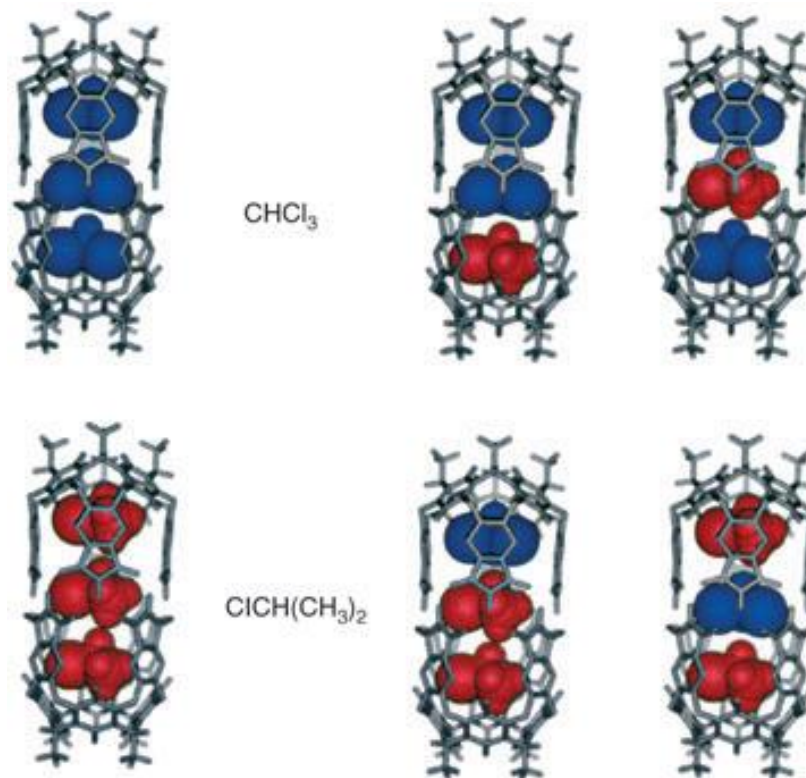
The orientational preference of one guest depends on the presence of the co-guest.



MM optimized structures:
chloroformio e *para*-etiltoluene



Constellation Isomers



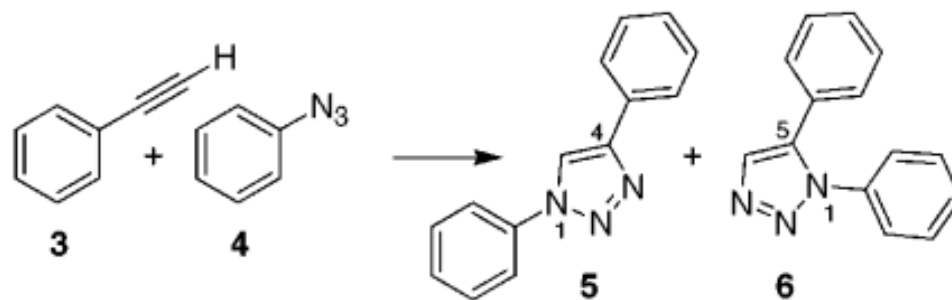
MM optimized structures:
cloroformio e *iso*-propilcloruro

In addition to being able to preserve highly labile species, they may serve as catalysts and accelerate reactions inside their inner cavity by either concentrating the reactants leading to higher effective concentrations or TS stabilization or by preorganising them inside the capsule.

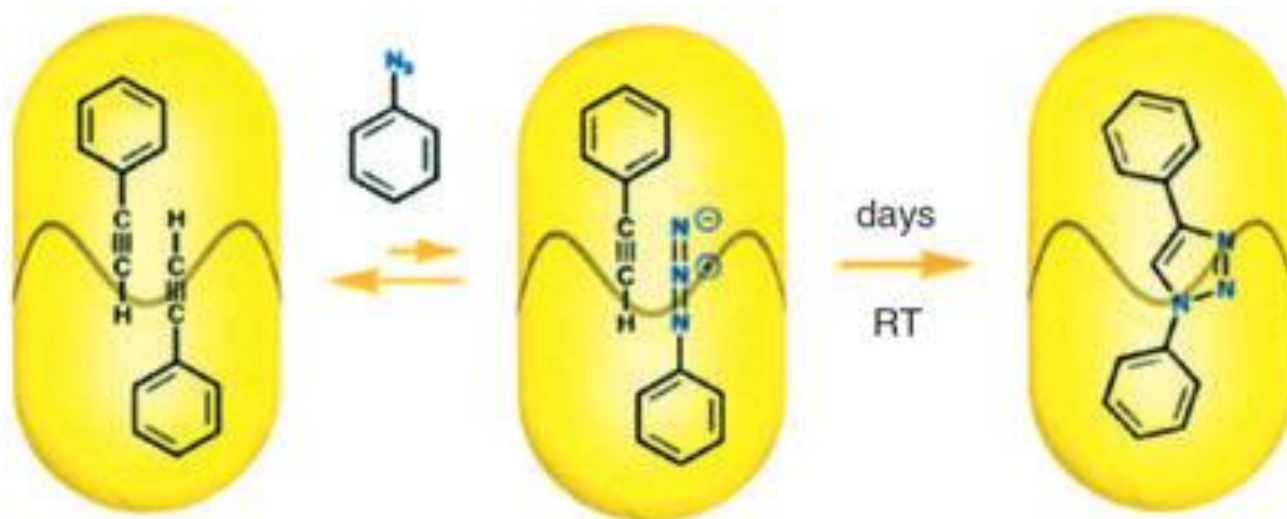
They may create a micro-environment in which two encapsulated reactants are held together in a orientation that differs from their most reactive arrangement in solution (or gas phase) leading to products that are disfavoured in equivalent solution phase reactions.

Reattività nelle capsule molecolari

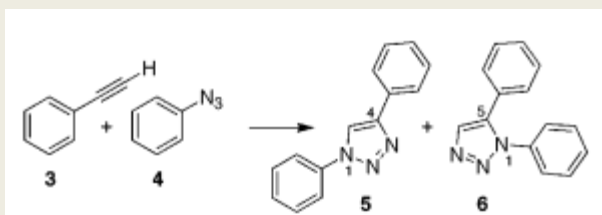
Cicloaddizione 1,3 regioselettiva di fenilacetilene e fenilazide



Reattività nelle capsule molecolari



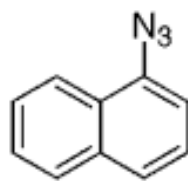
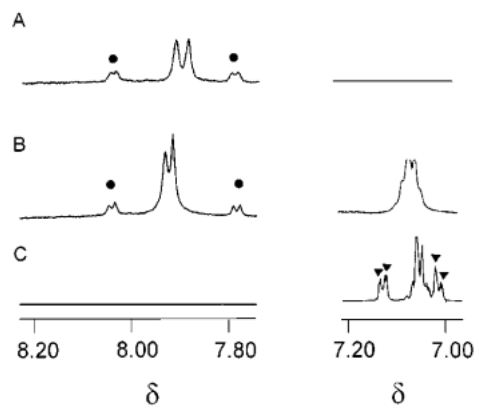
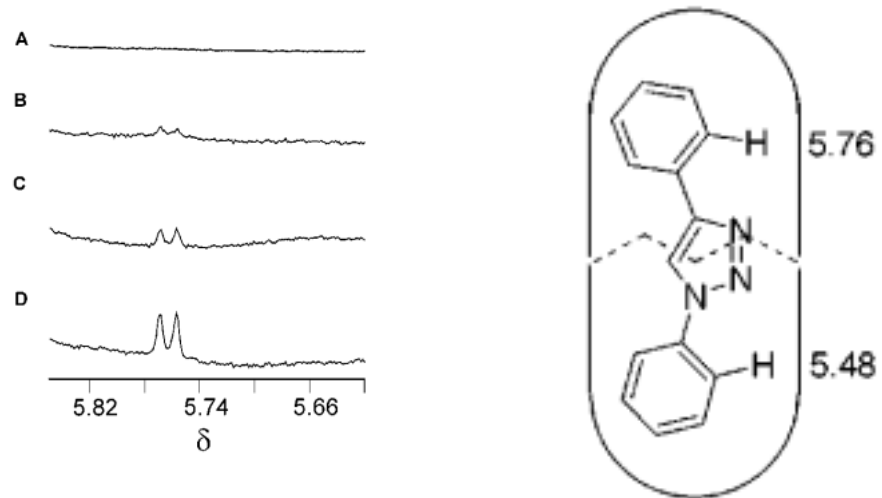
Cicloaddizione 1,3 regioselettiva di fenilacetilene e fenilazide:



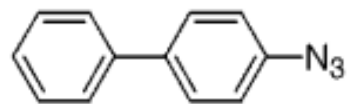
Volume definito = [] 4M vs mM

Tempo di contatto = 1 s vs 1 ns

Solvatazione fissa



7



8

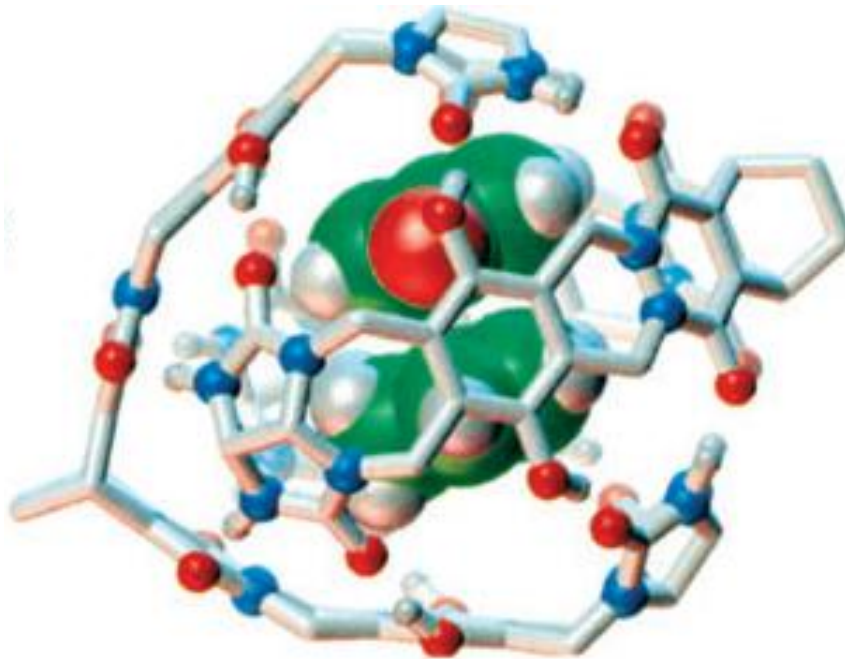
Reattività nelle capsule molecolari

Cicloaddizione Diels-Alder accelerata di ca. 200 volte

[] = 5M

Solvatazione

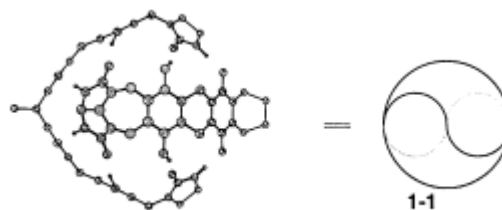
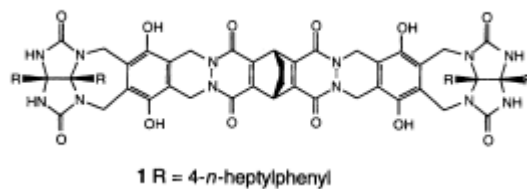
Tempo di contatto



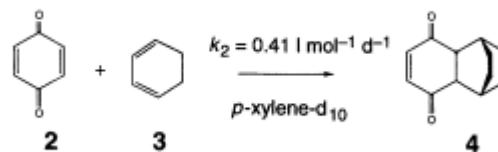
Acceleration of a Diels–Alder reaction by a self-assembled molecular capsule

Jongmin Kang & Julius Rebek Jr

NATURE · VOL 385 · 2 JANUARY 1997



(1)



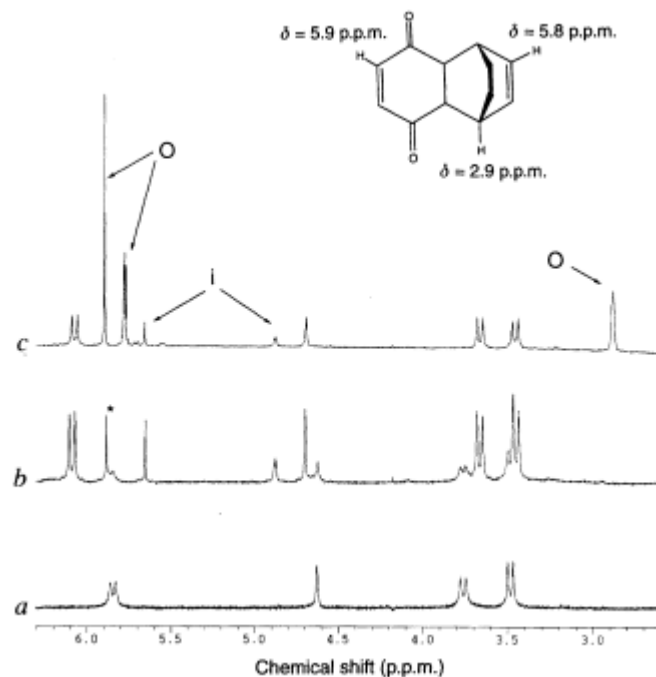
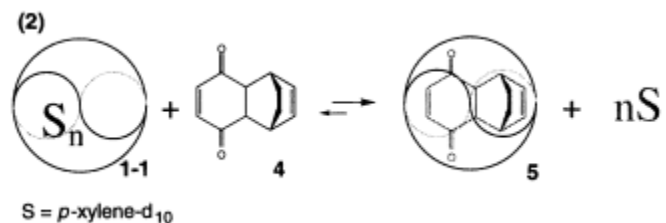


FIG. 2 Proton NMR spectra of **1-1** and its encapsulation complex with the adduct **4** in *p*-xylene- d_{10} . Signals of the guest inside the capsule and outside (free) are labelled with 'i' and 'o', respectively. The signal designated with an asterisk represents chloroform. a, Compound **1-1** alone. b, Compound **1-1** with 0.7 equiv. of Diels-Alder adduct **4** added; all of the latter is encapsulated and separate signals are observed for the complex **5** and solvated dimer **1-1**. c, Compound **1-1** with 6 equiv. of Diels-Alder adduct **4** added; all of the capsule is occupied as complex **5** and separate signals are observed for free and encapsulated adduct **4**. Assignments for resonances of free **4** are shown on the structure.

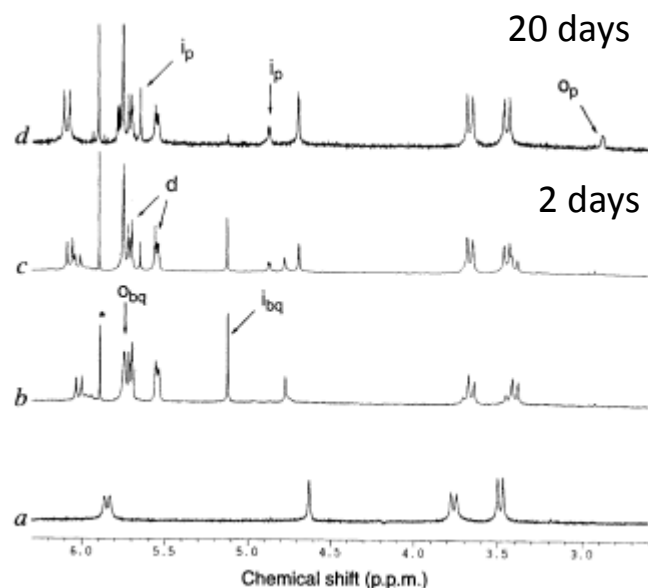
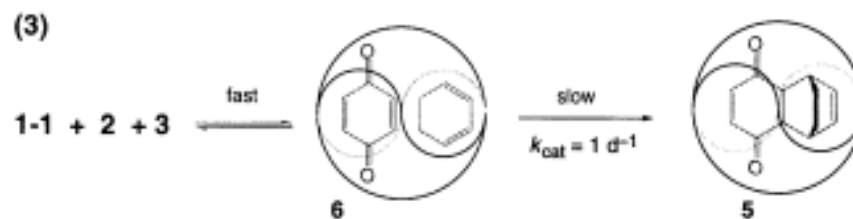


FIG. 3 Changes in the proton NMR spectra of **1-1** during the reaction of *p*-benzoquinone **2** and 1,3-cyclohexadiene **3** in *p*-xylene- d_{10} . The signals for *p*-benzoquinone(bq) and Diels-Alder product (p) inside and outside are designated as 'i' and 'o' respectively. Signals from cyclohexadiene are designated as 'd'. The signal designated with an asterisk represents chloroform impurity. a, Compound **1-1** alone. b, Shortly after 4 equiv. of *p*-benzoquinone and 4 equiv. of 1,3-cyclohexadiene were added to the solution of **1-1**. c, The reaction mixture after 2 days. d, The reaction mixture after 19 days, showing evidence of released product and **5** as the principal species.

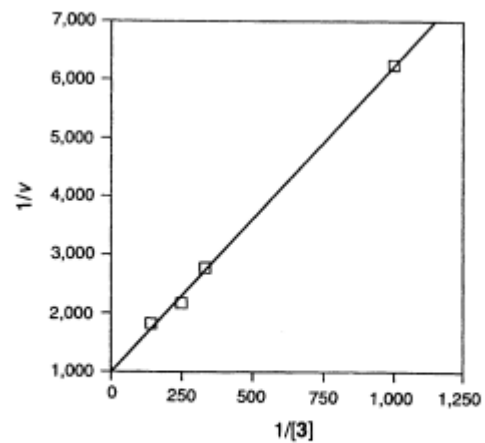
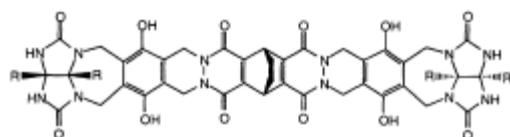
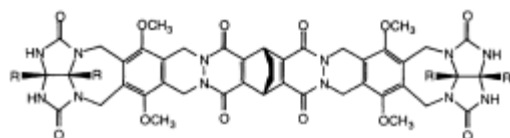


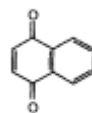
FIG. 4 Lineweaver-Burke plot of the reaction rates, V , of **2** with **3** in the presence of **1-1**. The concentrations of 1,3-cyclohexadiene **3** were changed with a constant concentration (4 mM) of *p*-benzoquinone.



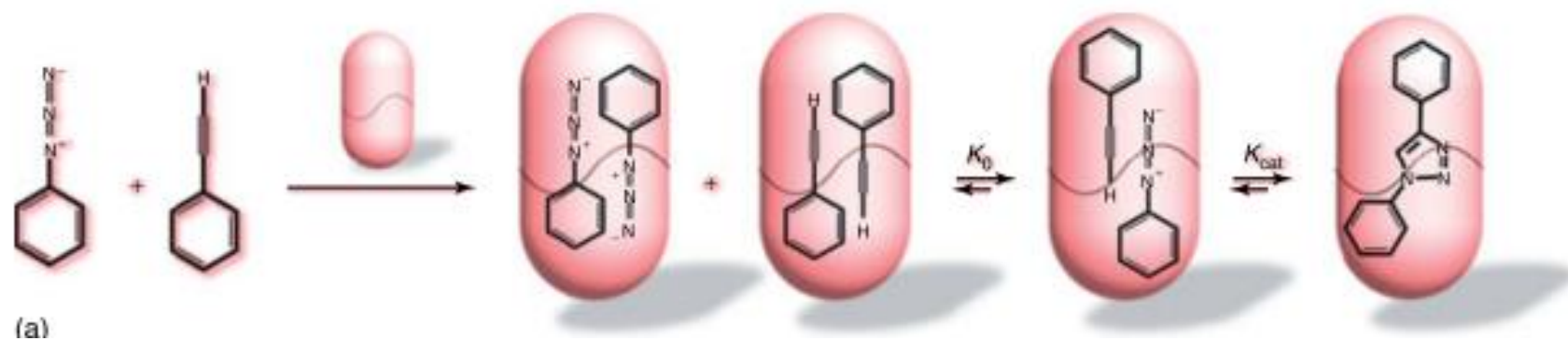
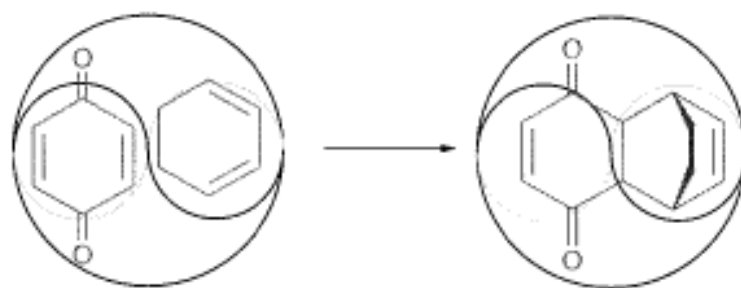
9 R = 4-*n*-heptylphenyl



10 R = 4-*n*-heptylphenyl



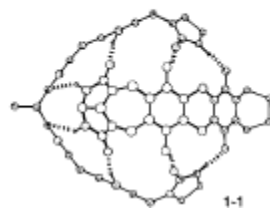
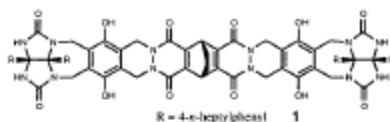
11



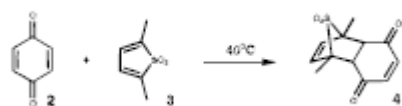
Self-Assembled Molecular Capsule Catalyzes a Diels–Alder Reaction

J. Am. Chem. Soc. 1998, 120, 7389–7390

Jongmin Kang, Javier Santamaria, Göran Hilmersson, and Julius Rebek, Jr.*



Scheme 1



Scheme 2



Scheme 3

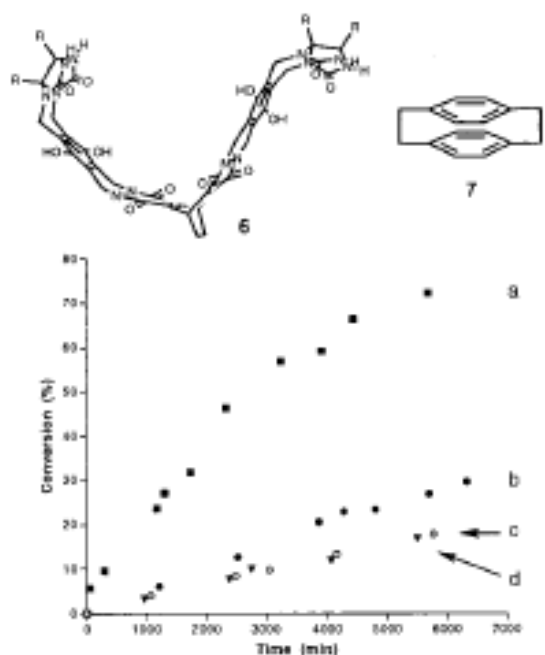
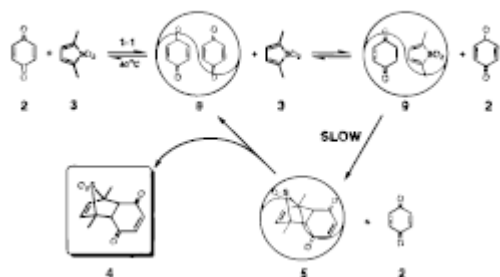


Figure 2. Comparative study of the formation of the Diels–Alder adduct along the time: (a) catalyzed reaction; (b) reaction inhibited with 1 equiv (with respect to the softball) of [2,2]paracyclophane (7); (c) background reaction; (d) use of S-shaped isomer 6 instead of hydroxy softball.

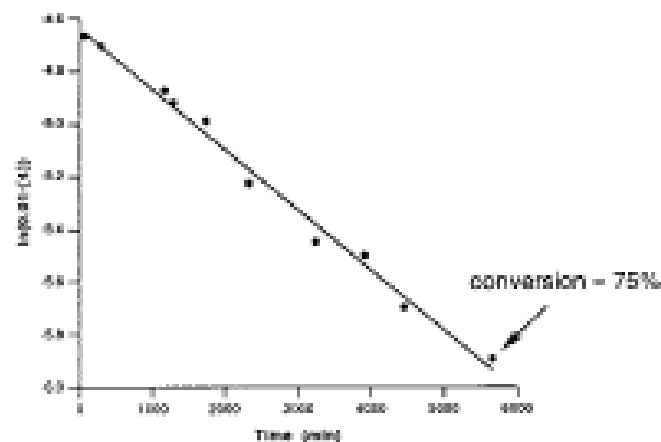


Figure 3. Logarithmic plot of the formation of the Diels–Alder adduct using hydroxy softball as catalyst. It shows linearity over 75% conversion. The experiment has been performed in *p*-xylene-*d*₁₀ at 40 °C, with concentrations of 10 mM for the reactants and 1 mM for the capsule.

